Development of a Transformer-Based Electrical Stimulation Driver for a Wearable Physiotherapy System

João Lucas Gonçalves - 37887

Dissertação apresentada à Escola Superior de Tecnologia e de Gestão de Bragança para obtenção do Grau de Mestrado em Engenharia Industrial (Engenharia Eletrotécnica).

Trabalho orientado por:

Prof. José Lima

Prof. José Augusto Carvalho

Esta dissertação não inclui as críticas e sugestões feitas pelo Júri.

Bragança

2022/2023

Development of a Transformer-Based Electrical Stimulation Driver for a Wearable Physiotherapy System

João Lucas Gonçalves - 37887

Dissertação apresentada à Escola Superior de Tecnologia e de Gestão de Bragança para obtenção do Grau de Mestrado em Engenharia Industrial (Engenharia Eletrotécnica).

Trabalho orientado por:

Prof. José Lima

Prof. José Augusto Carvalho

Esta dissertação não inclui as críticas e sugestões feitas pelo Júri.

Bragança

2022/2023

Dedication

To my family that support me from far away.

Acknowledgements

I would like to express my gratitude to several individuals who have made invaluable contributions to this project. First and foremost, I would like to extend my sincere appreciation to my supervisors, Professor José Lima and Professor José Augusto Carvalho, at the Polytechnic Institute of Bragança. As a master's student, Professor Lima and Professor Carvalho provided me with guidance and advice throughout this project.

I am also thankful to Professor Paulo Leitao, also from the Polytechnic Institute of Bragança. Professor Leitao offered me the opportunity to become part of this development project and introduced me to the world of academic research.

Last but certainly not least, I am deeply grateful to my colleagues Tiago Franco, Leonardo Sestrem, and Raul Kaiser. They provided valuable assistance on various aspects of this work, particularly in areas where my expertise was limited. Their contributions were instrumental in the implementation and testing of this project.

Abstract

This work presents the development of an electrical stimulation driver for two wearable systems: NanoStim and NanoID. These systems are designed for physiotherapy purposes, with NanoStim focusing on the treatment of knee pathologies and NanoID on balance control. The goal of this work is to create a compact electrical stimulation driver with low processing consumption capable of inducing muscle contractions in a wide range of applications. The proposed solution involves the development of two transformer-based stimulation drivers, each controlled by a microcontroller and a mobile application. These drivers are based on distinct transformer models, each tailored to produce muscle contractions through the application of electrical pulses and are designed to meet the requirements for integration into wearable systems. Both alternatives underwent testing and validation with volunteers, and the collected data was analyzed to determine the optimal circuit alternative for implementation in both wearable systems.

Keywords: Electrical Stimulation, Functional Electrical Stimulation, Electrical Stimulation Circuit, Wearable System.

Contents

List of Tables

List of Figures

Acronyms

I^2C Inter-Integrated Circuit. 15

R_{DS} Drain-Source Resistance. 21

V_{GS} Gate Threshold Voltage. 21

BLE Bluetooth Low Energy. 19, 32, 33

BMI Body Mass Index. xvi, 46–50

DAC Digital Analog Converter. 12

DSP Digital Signal Processor. 12

ECG Electrocardiogram. 3

EMG Electromyography. 3

ES Electical Stimulation. 3–6, 8, 47

FD Foot drop. 5, 12

FES Functional Electrical Stimulation. xi, xv, 4–7, 9, 12, 53, 54

GPIO General Purpose Input/Output. 34, 35

IMU Inertial Measurement Unit. 3, 15, 32

IoT Internet of Things. 14

MOSFET Metal-Oxide-Semiconductor Field Effect Transistor. 21, 23

MQTT Message Queuing Telemetry Protocol. 15

PCB Printed Circuit Board. 26, 27

PCMC Peak Current-Mode Control. 13

PWM Pulse Width Modulation. 12–15, 23, 32–37, 53

SSO Single Sign-On. 31

Chapter 1

Introduction

Muscle atrophies are among the primary causes of muscle dysfunction, a condition that can lead to impaired movement in individuals, making everyday tasks challenging or even impossible to perform. This condition can arise from various circumstances, each with varying levels of complexity. Muscle impairment may result from a spinal cord injury, leading to a total or partial loss of sensory function. It can also be caused by permanent disability resulting from a stroke or muscle deterioration associated with aging-related pathologies [1][2][3][4].

With this in mind, in addition to the typical therapy methods employed in physiotherapy treatments, electrical stimulation is one of the most commonly used techniques to enhance the mobility of patients suffering from these conditions. Essentially, electrical stimulation is a method that involves the application of electrical pulses to induce muscle contractions. While this method can be employed in various modalities, the application discussed in this project is related to functional activities, known as Functional Electrical Stimulation. This modality combines the use of electrical stimulation with functional activities to generate desired movement patterns, thus aiding in the rehabilitation and treatment of motor skills that have been compromised or lost due to various pathologies [2][1][5].

In this context, this project introduces and presents the development of a Functional Electrical Stimulation Driver designed to produce electrical stimulation pulses within a wearable device intended for physiotherapy applications. This application necessitates a compact driver

capable of delivering stimulation across a wide range of scenarios. To address this, the proposed solution comprises two options of stimulation circuits, each based on a different type of transformer. Both circuits are controlled by a microcontroller, which receives commands from a mobile application.

1.1 Motivation

The development of this work took place during the execution of the projects NanoStim and NanoID. Both projects aim to create a wearable physiotherapy device capable of real-time feedback stimulation based on the acquisition of electromyography (EMG) signals and a position sensor. In the NanoStim system, the primary focus is on treating knee pathologies, while the NanoID system focuses on balance treatment. The difference in applications between both projects results in varying numbers of sensors and actuators implemented in each system, although they operate in a similar manner. NanoStim requires fewer components to fulfill its intended function since it targets a single muscle for treatment. On the other hand, NanoID deals with multiple muscles to achieve its posture and balance objectives, which necessitates a larger number of components. The architecture of both systems can be observed in Figure 1.1 and Figure 1.2.

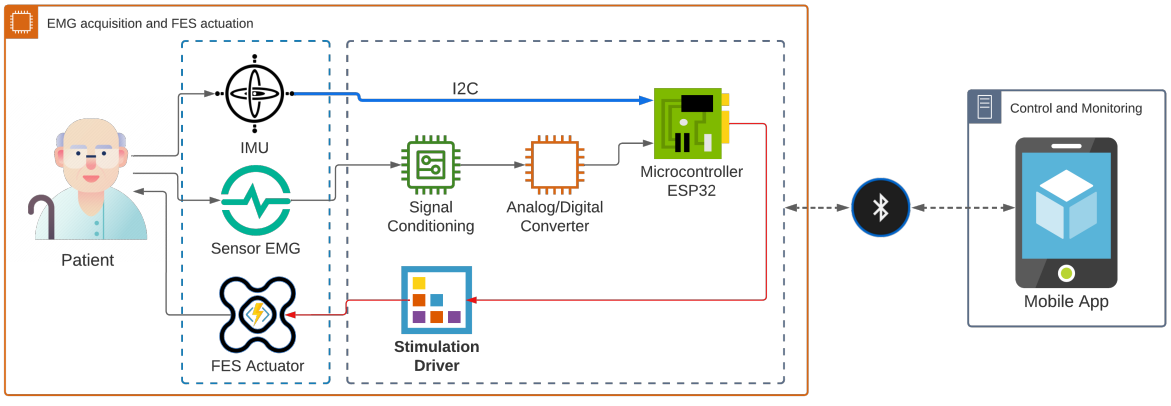

Figure 1.1: NanoStim Architecture

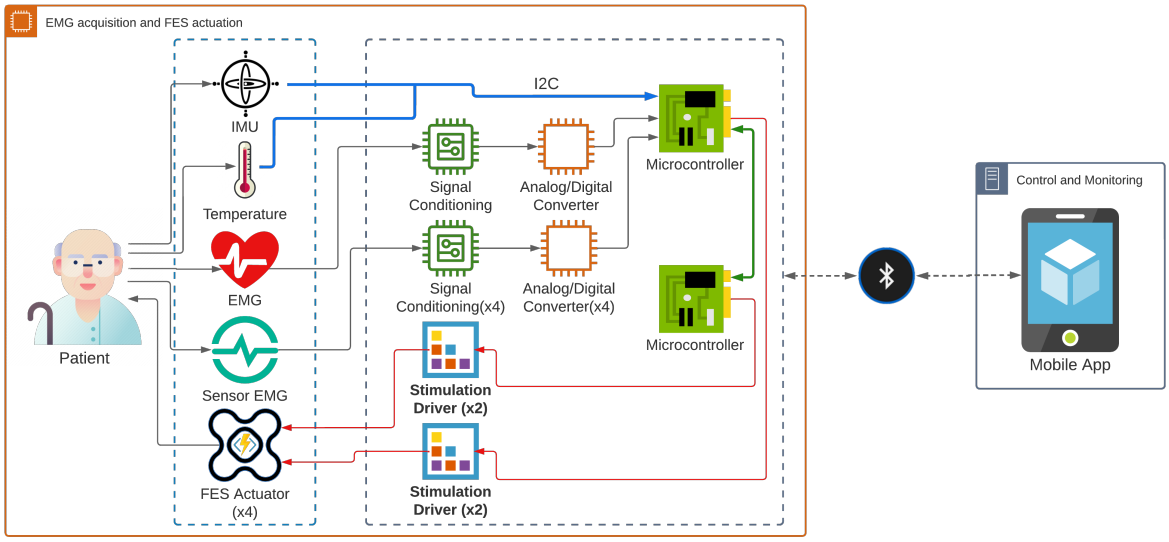

Figure 1.2: NanoID Architecture

It is evident that the elements comprising both architectures are the same, varying in quantity. The NanoStim architecture includes one of each element, which consists of a microcontroller, a stimulation driver, an Electromyography (EMG) sensor, and an Inertial Measurement Unit (IMU) sensor. On the other hand, the NanoID architecture incorporates a greater number of elements, including two microcontrollers, four stimulation drivers, four EMG sensors, one Electrocardiogram (ECG) sensor, one temperature sensor, and one IMU sensor. Both systems are controlled by a mobile application, which receives information acquired from the sensors and sends commands to the actuators.

1.2 Problem and Objectives

Having established the project framework, the problem addressed in this work involves the development of an Electical Stimulation (ES) driver for the NanoStim and NanoID wearable systems. The driver must possess the capability to generate stimulation signals effective in inducing muscle contractions while allowing for extensive parameter control. Ideally, the stimulation signals must be biphasic, with a 50Hz maximum frequency and 250-300 s of maximum

pulse duration. Moreover, the driver must have a compact form factor suitable for integration into a wearable device and must prioritize the comfort of the patient during stimulation treatment. Taking into consideration these factors, the objective of this work is to conceptualize, develop, and validate two transformer-based Electrical Stimulation drivers for use in a physiotherapy wearable solution.

1.3 Document Structure

This document is structured as follows: Chapter 2 provides an introduction to the theoretical fundamentals of ES and FES, emphasizing the essential functions that the driver must possess to facilitate stimulation. It also reviews the state of the art in previous works related to electrical stimulation circuits. Chapter 3 details the circuit development, reiterating the problem addressed in this work and offering an in-depth description of the problem and proposed solutions. It emphasizes the materials and methods employed, focusing on the description and implementation of the proposed alternatives. Chapter 4 covers the software development of the driver, outlining the software architecture of the system and describing the configuration, generation, and control of stimulation signals. It highlights the necessary steps for setting up the tools used for pulse generation and control. Chapter 5 discusses the tests, results, and evaluations employed to validate the operation of the proposed circuits. Finally, Chapter 6 provides a summary and conclusion of the work, along with suggestions for future research.

Chapter 2

State of the art

This chapter aims to provide an overview of the theoretical fundamentals, the physiological context, and the technical applications of the primary concepts presented in this work. It begins with a description of FES, including its operation, applications, and contextualization based on physiological principles. Following that, it delves into the technical fundamentals of FES applications, including approaches to its operation and design. Finally, a discussion of related works focusing on the development and application of FES systems is presented.

2.1 Functional Electrical Stimulation (FES)

FES is a method employed to supplement or replace functions of the sensory-motor system by applying short electrical pulses [1][6][7][5]. FES systems find application in the treatment and rehabilitation of stroke patients suffering from Foot drop (FD) cases [8][9][7], hemiplegia (unilateral arm and/or leg paralysis) [10][7], control of standing and walking [11][12][7], and restoration of function in chronic applications to prevent muscle atrophy [6][5].

This method of ES represents a specific therapeutic application. ES methods induce physiological changes through the application of electrical pulses aimed at enhancing tissue health or voluntary function [5]. In contrast, FES is focused on facilitating motion by synchronously or intermittently pairing the stimulus with a voluntary activity, thereby replacing or assisting voluntary movement. Consequently, FES systems are designed to be used or worn by the patient

[13][5].

The application of FES involves delivering a series of short electrical pulses to nerves, which trigger the generation of action potentials [7][5]. Stimulation electrodes generate a localized electrical field that facilitates the depolarization of neuronal cell membranes. Once the depolarization reaches a certain threshold, it initiates an action potential that propagates both towards and away from the stimulation site. Action potentials that propagate near the peripheral nerve axons dissipate within the body's cells, while those that propagate further from the point of stimulation are conducted through the neuromuscular junction, resulting in muscle fiber contraction. Interestingly, in contrast to the physiological principle where small motor units are typically activated first, larger muscle units (innervated by larger-diameter axons) can be activated with less current, a phenomenon known as reverse recruitment [5][1][14].

Motor functions generated by FES applications are rooted in the principle that ES primarily activates neurons rather than muscle fibers. This is because the amount of charge required to elicit action potentials in neurons is significantly lower than what is needed to provoke action potentials in muscles. Consequently, the effectiveness of FES applications hinges on the integrity of both the muscle and the neuromuscular junction [5].

2.2 FES technical fundamentals

The development of a FES system requires the assimilation of a set of technical fundamentals. These fundamentals define the essential functions that the stimulation driver must fulfill to effectively induce muscle contractions.

The technical fundamentals of a FES system encompass electrode placement and pulse characteristics. Electrode placement dictates which muscles will be activated, while pulse characteristics determine the intended therapeutic effects.

2.2.1 Electrode Placement

The electrical stimulus can be delivered to the tissue through electrode systems placed on the skin surface, delivered percutaneously, or implanted directly into the target muscle [5][15][1].

Surface or transcutaneous electrodes are positioned on the patient's skin, directly over the nerves or at the muscle's "motor point," which is the most optimal location for generating isolated muscle contractions with minimal intensity. The primary advantage of this system lies in its ease of application, thanks to its noninvasive nature. However, it can be challenging to stimulate deep muscles, and improper preparation or placement of the electrode may lead to skin irritation or damage [5][15].

Percutaneous systems involve the use of intramuscular electrodes that are implanted directly into the muscles, penetrating through the skin and positioned in proximity to the nerves. These electrodes are inserted into the muscle using a needle that passes through the skin, allowing them to access deeper muscles and necessitating lower intensity to induce muscle contractions. This technique is considered minimally invasive but requires special preparations to mitigate potential complications [5][15].

Implanted systems are stimulators implanted via open surgery directly onto the target muscle or nerve. These systems are designed for long-term use but are highly invasive. Various electrode configurations can be implanted to suit each specific case. These implants may be positioned at different locations within the muscle and require specific types of electrodes, such as epimysial electrodes for the muscle surface, intramuscular electrodes within the muscle tissue, epineural electrodes adjacent to a nerve, and cuff electrodes encircling the nerve (helix or cuff electrodes). Implantable circuits composed of intramuscular electrodes allow for the activation of smaller or deeper muscles. However, it's important to note that this invasive option is typically reserved for specific circumstances [5][15].

2.2.2 Pulse Characteristics

Muscle contraction is initiated by stimulation pulses, which are waveforms defined by three key parameters: frequency, amplitude, and duration. These parameters play a critical role in

determining the strength of muscle contraction and the type of treatment provided. The subsequent subsections will elaborate on the pulse characteristics responsible for generating muscle contractions [5][1][2][3].

Waveform Selection

Pulse waveforms typically come in monophasic and biphasic shapes. Monophasic waveforms consist of a series of unidirectional pulses, delivering current in only one direction. Biphasic waveforms, on the other hand, are comprised of two phases, with a positive phase followed by a negative one [5][2].

Using monophasic pulses exclusively has the potential to result in electrode degradation and tissue damage when applied over extended periods. This occurs due to an electrochemical process that alters the ionic distribution within the skin, leading to polarization, which, in turn, may result in tissue breakdown and burns. The introduction of biphasic pulses serves the purpose of reversing this process by promoting tissue depolarization, thereby enabling stimulation without causing harm to the tissue [5][2][3].

The total charge delivered to the tissue is calculated by measuring the area under each pulse within its period. Waveforms can be classified as either balanced or unbalanced, with balanced waveforms featuring positive and negative pulses that distribute equal areas, whereas unbalanced waveforms have pulses with varying areas. In practice, the balanced waveform, where the positive and negative phases have equal areas, is more frequently employed. Consequently, for most ES applications, the biphasic symmetrical waveform is the preferred choice [5][2][3].

Stimulation Parameters

The stimulation waveform is defined by three key parameters: frequency, amplitude, and duration, which collectively determine the characteristics of muscle contraction [5][3].

The stimulation frequency plays a pivotal role in shaping the quality of muscle contraction and influencing muscle fatigue. At low pulse frequencies, the muscle response manifests as a

series of twitches. Once the frequency surpasses a specific threshold known as the fusion frequency, the muscle response transitions into a smooth, sustained contraction. Repeated stimuli within a given timeframe result in a cumulative effect referred to as temporal summation. On the other hand, high stimulation frequencies can impact the intensity of muscle contraction, although they also lead to an increase in muscle fatigue [5][3].

The intensity level and pulse duration needed to trigger muscle contractions can vary significantly among individuals, and the strength of the contraction is determined by the number of motor units recruited by the pulse. The electrical field generated by the pulse is responsible for recruiting motor units. The total charge delivered to the muscle is dictated by the pulse's amplitude and width. To induce muscle contraction, the applied pulse is precisely controlled in terms of both amplitude, measured in volts, and duration, measured in microseconds [5][3].

2.3 Literature Overview

This section is dedicated to presenting and analyzing works related to the proposed project's development. The following segment aims to investigate various approaches to the problem and compare these solutions, with the goal of establishing a theoretical foundation for the project's development.

The presented works are centered on the development of output circuits for FES. This literature analysis describes the author's chosen approach, the components utilized, and the operation of each proposed system.

Related Works

CHENG et al. (2004) [16], propose two alternatives capable of generating stimulation pulses controlled in duration, frequency, and amplitude. The first circuit, shown in Figure 2.1, comprises two integrated circuit timers, both 555 timers. The first timer is configured as monostable, while the second operates in an astable configuration to generate the output pulse train. Adjusting the values of the resistors (R_1, R_A, R_B) and capacitors (C_1 and C_2) controls pulse duration and frequency. Four operational amplifiers are employed, with two (*OP1* and *OP2*) generating

the output signal, while the other two (*OP3* and *OP4*) form the current feedback loop to ensure the desired current amplitude. The pulse amplitude is regulated by R_2, and a transformer is used to step up the output voltage [16].

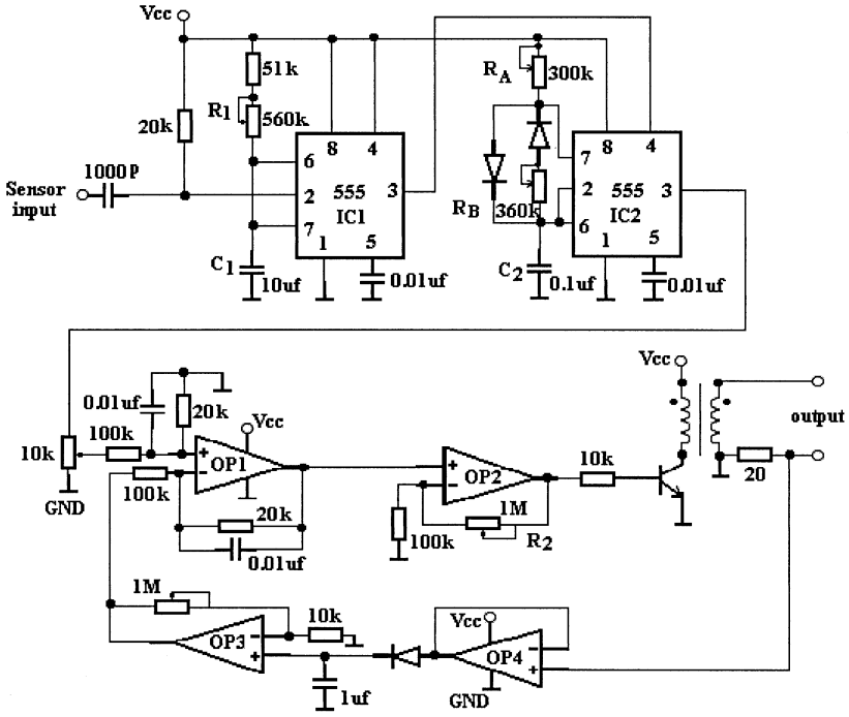

Figure 2.1: Transformer based circuit proposed by *CHENG et al.* [16].

The second circuit, as shown in Figure 2.2, is based on a resonant converter. It consists of two transistors, resonant components (C_1 and L_1), and amplitude regulator components (C_2, L_2, and R) [16]. This alternative allows for the generation of biphasic pulses.

Based on the first circuit proposed by CHENG *et al.*, VELLOSO *et al.* [17] presented a system controlled by a virtual instrument developed in *LabView 7.1*, applied using a USB device (USB 6501 - National Instruments). This setup allows the user to define the parameters for the electrical stimulation signals. The output stage, as shown in Figure 2.3, is composed of three operational amplifiers used for signal conditioning and feedback. It is followed by a pair of transistors employed to provide the necessary current for the transformer to step up the output signal [17].

Following a similar approach to the transformer application, CHEN *et al.* [18] proposed a

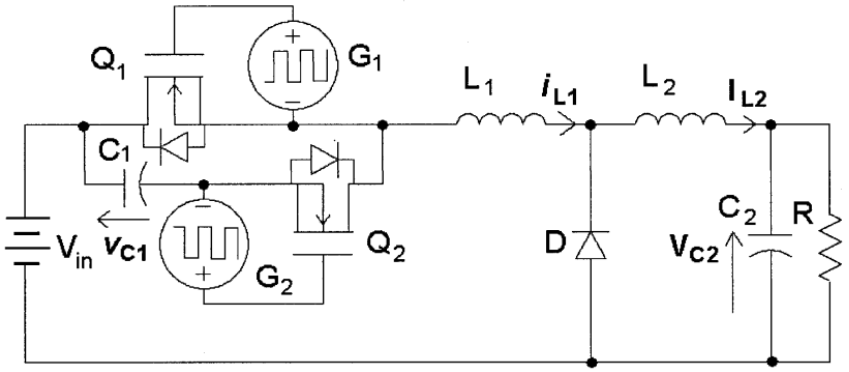

Figure 2.2: Resonant circuit proposed by *CHENG et al.* [16].

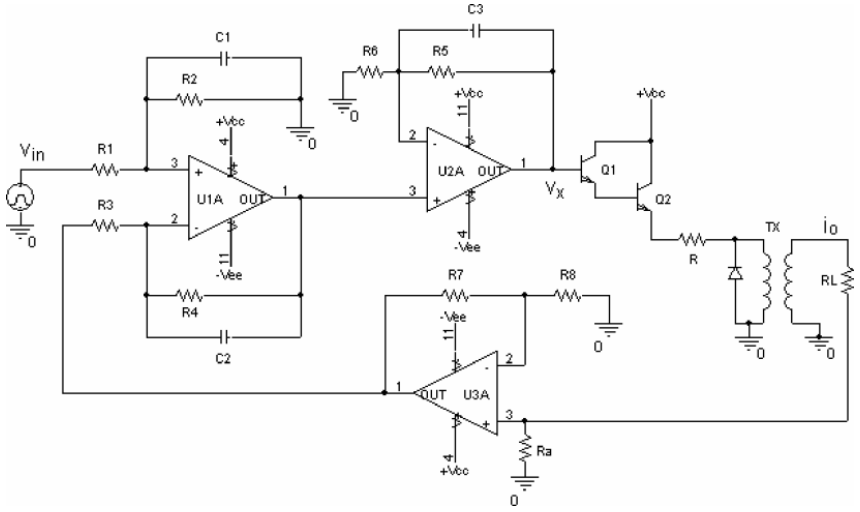

Figure 2.3: Output current driver circuit proposed by *VELLOSO et al.* [17]

circuit suitable for FD treatment. The system comprises a Digital Signal Processor (DSP) for controlling pulse generation, a pair of FES electrodes, and a heel pressure sensor. To generate rectangular pulses, the system employs Pulse Width Modulation (PWM), and a MOSFET is used to regulate the input current to the transformer, which amplifies the output voltage. The circuit proposed by CHEN *et al.* can be observed in Figure 2.4.

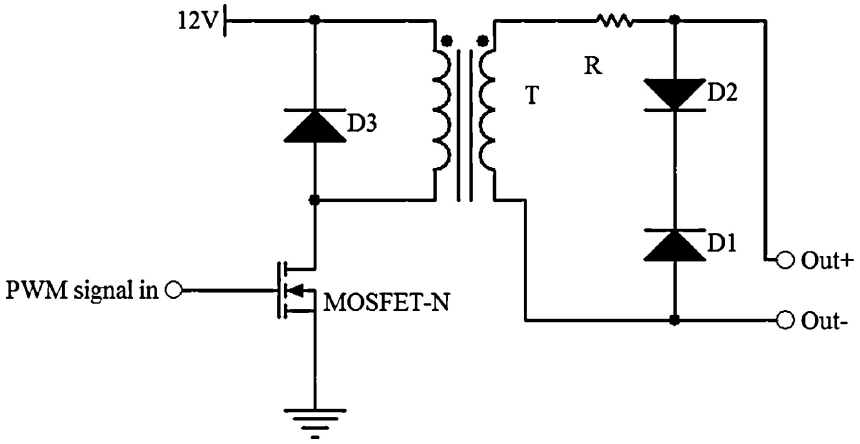

Figure 2.4: FES circuit proposed by *CHEN et al.* [18]

WANG et al. [3] propose a comprehensive control system based on a microcontroller as its core, responsible for controlling all the other components, including stimulation pulse generation. The pulse stimulation circuit they propose, depicted in Figure 2.5, receives two intercalated signals ($P_{1.7}$ and $P_{1.6}$) from the microcontroller. It employs two sets of transistors (Q_2, Q_3, Q_6 and Q_1, Q_4, Q_5) to generate biphasic pulses, while intensity regulation is achieved using Pulse Width Modulation (PWM). When $P_{1.7}$ is set to high, Q_2, Q_3, Q_6 are activated, allowing current to flow from Q_2 to the electrodes and then be received by Q_3. Similarly, when $P_{1.6}$ is set to high, current flows from Q_1 to the electrodes and is received by Q_4, resulting in the generation of biphasic pulses [3]. This circuit can be observed in Figure 2.5.

MASDAR *et al.* [2] introduced a device built around a microcontroller, a wireless system employing a Zigbee module, and a voltage-to-current converter circuit designed for generating both monophasic and biphasic pulses for FES applications. The output circuit utilizes a voltage-current converter that relies on a power operational amplifier (LM675). Controlled by the Zigbee wireless network, the microcontroller manages voltage control through a Digital

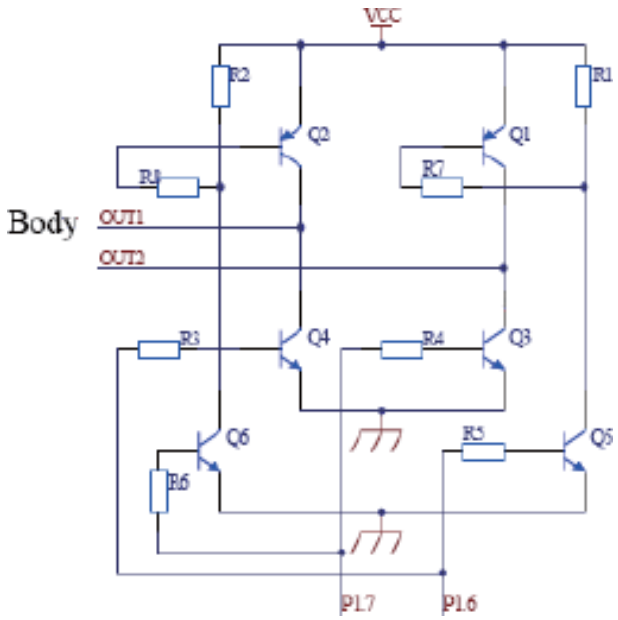

Figure 2.5: Stimulation Pulse Generating Circuit, proposed by *WANG et al.* [3]

Analog Converter (DAC), which is then converted to current and amplified by the operational amplifier.

H.P. WANG *et al.* [19] introduced a four-channel pulse-triggered stimulation system capable of generating four biphasic pulses. The system employs a microcontroller to establish a queuing algorithm for an H-bridge configuration and a four-channel multiplexer to enable time-division output. The hardware consists of both a low-voltage and a high-voltage side. The low-voltage side includes two transconductance amplifiers based on the Holland structure, resistors, and an operational amplifier drift-removing circuit. On the other hand, the high-voltage side comprises a pair of complementary Wilson current mirrors.

SHIRAFKAN *et al.* [20] have proposed a current-based stimulation circuit consisting of a flyback converter, an H-bridge, a sensor network, and a PWM controller. This system achieves output current regulation by employing a Peak Current-Mode Control (PCMC) flyback configuration that senses the converter's output voltage to determine the PWM duty cycle. The biphasic pulses are generated by the H-bridge, which receives the PWM signal after amplification by a transformer, following the feedback loop of the control circuit. The stimulation output circuit proposed by the author can be seen in Figure 2.6.

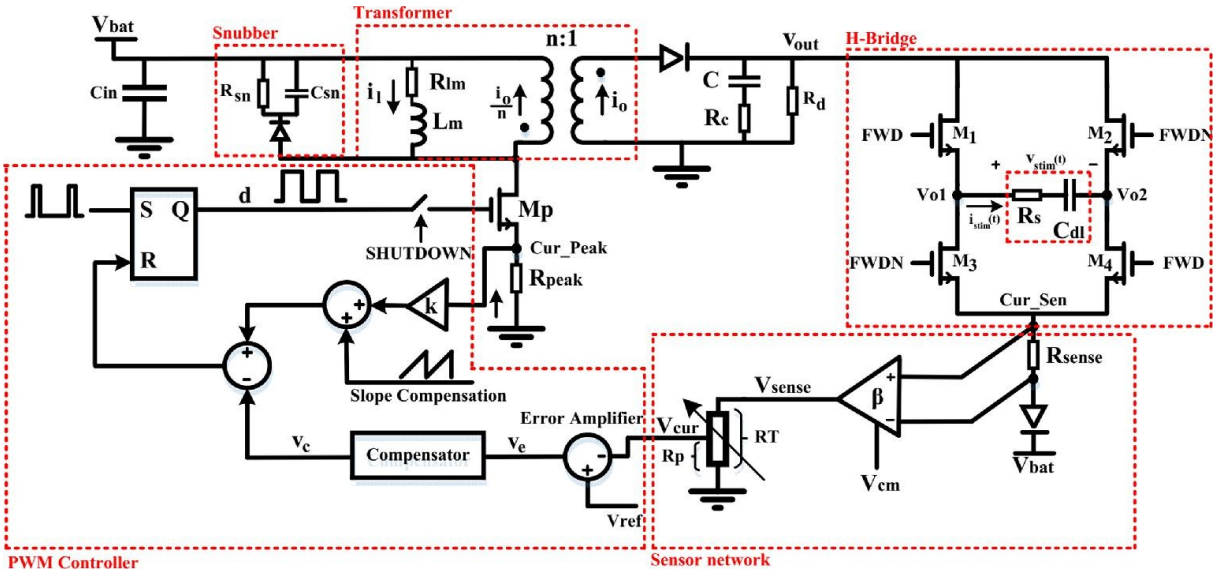

Figure 2.6: Stimulation and control circuits, proposed by SHIRAFKAN *et al.* [20]

BASUMATARY *et al.* [21] have presented a system comprised of an ESP32 microcontroller, pulse converter, amplifier circuit, and a power supply. In this configuration, the ESP32 generates two uniphasic signals, which are subsequently converted into a biphasic output using an instrumentation amplifier. This biphasic signal is then directed through an operational amplifier and a pair of transistors to buffer the current. Finally, the output signal is amplified by a transformer [21].

SANTOS *et al.* [22] have introduced an electrical stimulation system based on a step-up converter, an H-bridge unit controlled by a microcontroller, and a user-friendly software interface. This software interface enables users to control various stimulation parameters, including the electrical stimulation modality, session duration, waveform phase (monophasic or biphasic), pulse frequency, pulse duration, and current intensity. The software, in turn, commands a microcontroller unit responsible for generating PWM commands based on the configured parameters. The step-up converter is responsible for setting the pulse amplitude, while the H-bridge configuration is utilized to implement the time-related parameters established through the software [22].

ALMEIDA *et al.*[23] proposed a 4-channel Internet of Things (IoT) electrostimulator device equipped with an inertial sensor. The electrostimulation system consists of four modules: Boost

Converter, H-bridge, IMU, and Processing Module. The Processing Module is centered around an ESP32 microcontroller that utilizes the Message Queuing Telemetry Protocol (MQTT) communication protocol. This module manages the stimulation boost voltage, signal modulation via PWM signals, and extracts data from the IMU using the Inter-Integrated Circuit (I^2C) protocol. The stimulation circuit comprises the Boost Converter and the H-bridge, where the boost converter amplifies the input voltage set by the PWM, and the H-bridge generates the stimulation waveforms.

Chapter 3

Circuit Development

This chapter commences by introducing the problem under investigation, offering a comprehensive description of the challenges and complexities involved. Subsequently, the proposed solutions are presented, introducing the overall architectures and distinct approaches of the two proposed solutions. Following this, the Materials and Methods applied for the development of these solutions are outlined. Lastly, the chapter delves into the development and implementation of both circuits, providing an in-depth explanation of the development process, the circuit description, and their successful implementation.

3.1 Problem Characterization

The problem at hand involves the development of a single electrical stimulation circuit designed to cater to two distinct applications. Both applications are intended for physiotherapy purposes, each addressing different treatment needs. The first application (NanoStim) focuses on treating knee pathologyes, while the second application (NanoID) is dedicated to fall prevention.

To meet the demands of these two applications, the stimulation circuit must possess a series of essential functions. It must be capable of generating muscle contractions through the precise application of electrical pulses. These pulses need to be generated and controlled through a mobile application, providing users with maximum flexibility and control over the system. Additionally, the circuit must maintain a compact form factor to fit seamlessly into a wearable

device while integrating harmoniously with the other functions of the system. This cohesive integration is essential to ensure effective and efficient performance for both applications.

3.2 Proposed Solutions

The proposed solutions consist of two circuits divided into three blocks: Control, Conditioning, and Amplification. Both circuits adhere to the same conditioning logic but differ in terms of control and amplification methods.

The overall architecture of the circuits comprises a microcontroller for command and control, a series of logic components for conditioning the input signals, and a step-up converter and a transformer for waveform output and amplification. The primary distinction between the circuits lies in the amplification block, where each solution adopts a different model of transformer. Due to the unique nature of functioning for each circuit, adjustments are made to the form of pulse generation and control.

To distinguish between the two solutions, they will be denominated by the type of transformer adopted in each circuit. The first solution is based on an **"isolation transformer"**, while the second solution utilizes an **"audio transformer"**.

3.2.1 Materials and Methods

After introducing and highlighting the problem at hand, the proposed solutions will be presented in detail. This will include a thorough explanation of the circuit architecture, encompassing its functional blocks: command, conditioning, and amplification. Each block's necessary functions will be outlined to ensure the proper results in accordance with the circuit's requirements. Furthermore, the materials and methods applied to meet these requirements will be described, accompanied by explanations for the application of each element used.

3.2.2 Circuit Architecture

The circuit architecture is organized into distinct functions performed by its elements. This division and classification are determined by the selected elements within each block. Throughout this chapter, these elements will be presented, along with their respective roles in the system. Furthermore, the rationale behind their selection within the given context will be thoroughly explained. By examining these aspects, this section aims to provide a comprehensive understanding of the circuit's design and its effective functioning within the specified applications.

Command Block

The first block, responsible for circuit control and command, comprises a microcontroller ESP32, which fulfills the control, command, and various other functions essential for the system's development.

The ESP32 was chosen for its powerful capabilities and cost-effectiveness, making it well-suited for embedded system applications. In the context of this project, it proves to be an ideal choice due to several factors. Firstly, its compatibility with the Arduino IDE framework allows for convenient programming with access to numerous function libraries. Additionally, the built-in wireless communication systems, especially the Bluetooth Low Energy (BLE) feature, provide the necessary connectivity for seamless communication with other devices. The ESP32's dual-core processor capability further enhances its value in this application, enabling efficient task handling and improved system performance. Furthermore, its low power consumption aligns perfectly with the project's energy efficiency objectives, ensuring optimal functionality even in power-constrained scenarios.

In this context, the ESP32 assumes the responsibility for communication, control, and command of the entire system, efficiently integrating all software components. The stimulation function is allocated in one core of the microcontroller, where the software generates the required pulse signals to execute the stimulation based on the application commands. The stimulation codes function by generating three types of pulses: two pulse trains modulated in time and one modulator pulse that determines the quantity and frequency of repetition. These pulses are

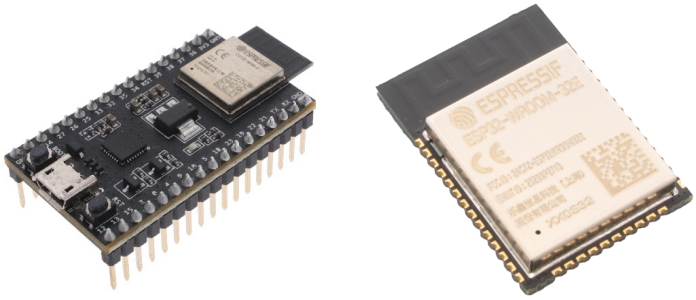

Figure 3.1: ESP 32 microcontroller.

then directed to the conditioning block, where they undergo logical operations before arriving at the amplification block as two pulses.

The approach to command and control is specific to each proposed stimulation circuit, resulting in distinct pulse production methods tailored to match each amplification block. The intricate software details will be explored extensively in Chapter 5.

Conditioning Block

The second block serves the role of signal conditioning and includes a **74LS08 AND** gate device, followed by a pair of N-type **30N06** MOSFETs. The **74LS08** device encompasses four independent gates, each dedicated to executing the logical **AND** function. Additionally, the block is enhanced with a duo of N-type **30N06** MOSFETs, employed for switching operations.

(a) **74LS08 AND** gates (b) **30N06** MOSFET

Figure 3.2: Illustrative images of the Command Block components.

The application of the **74LS08** involves transforming the three pulses generated by the Command Block into two pulses. The microcontroller generates two pulse trains in addition to a modulator pulse. These pulses are directed to the **AND** ports and are selectively merged based

on the modulator pulse using logical operations. An illustrative example of this application is depicted in Figure 3.3.

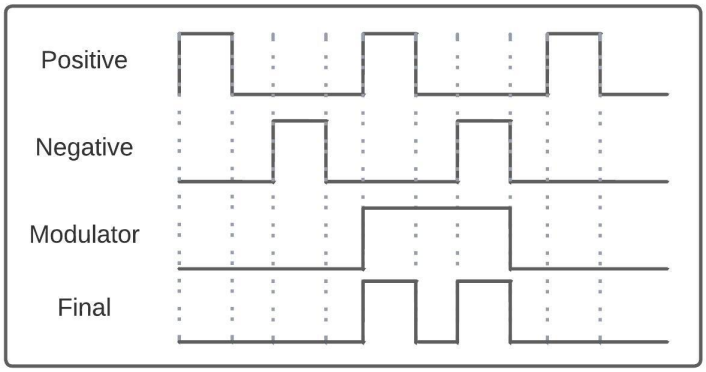

Figure 3.3: Example of the **AND** Gate Application.

The resulting pulses are transmitted to the Metal-Oxide-Semiconductor Field Effect Transistor (MOSFET) devices, which function as switches. For this purpose, N-type MOSFET model **30N06** was employed. This specific model was chosen due to its low Drain-Source Resistance (R_{DS}) of 0.035Ω. This characteristic is particularly significant because the pulse voltage value is 3.3V. Consequently, the switch voltage must remain below this threshold, taking into account that the Gate Threshold Voltage (V_{GS}) of this model ranges between *2.0V* and *4.0V*.

Amplification Block

Finally, the third block assumes the role of shaping the output pulse and handling amplification. This block consists of two essential components: a step-up converter and a transformer. In this context, the transformer plays a crucial role in generating the biphasic pulse form and further amplifying the pulses. Meanwhile, the step-up converter is tasked with providing sufficient energy to facilitate voltage amplification.

This block is subdivided into two distinct approaches, each revolving around a distinct transformer model. The initial approach is centered on the **Isolation transformer VB 0.5/2/6**, which is a *230V - 2 x 6V* transformer featuring dual outputs on the low-voltage side. With an operational frequency ranging from *50Hz to 60Hz*, it occupies dimensions of *22.7 by 22 by 19 mm*. This transformer configuration encompasses four pins on the low-voltage side and two pins

(a) Transformer VB 0.5/2/6

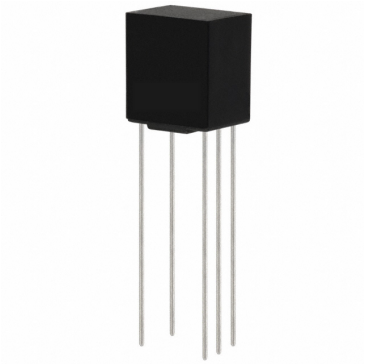

(b) Transformer MET-23

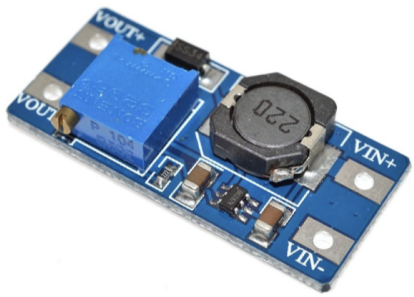

(c) Step-up MT3608

Figure 3.4: Amplification Block Components

on the high-voltage side, a pivotal arrangement for generating biphasic pulses. In this specific application, it serves as a step-up transformer.

The second approach is centered on the **Audio Transformer MET-23**. This transformer boasts a transformation ratio of *22.4:1V*, featuring three pins on the high-voltage side and two pins on the low-voltage side. Operating within a frequency range of *300Hz to 1KHz*, its dimensions measure *10.4 by 7.87 by 11.8mm*. However, due to the transformer's design as a step-up unit, its pin configuration is not as conducive to generating the biphasic shape. Given that the low-voltage side comprises only two pins, two units are utilized to fulfill the intended function.

The selection of these two options stems from their distinct advantages. While the first option offers relative simplicity in implementation, it suffers a notable drawback in terms of size and weight. In contrast, the second option is considerably smaller and lighter, despite necessitating the use of two units.

Regarding the Step-up converter, the model employed for this application is the **MT3608**. This component features an input voltage range spanning from *2V to 5.5V*, while the output voltage varies between *5V to 26V*. With dimensions of *30 by 17 by 14mm*, this converter effectively fulfills its designated function.

3.3 Circuit Description

The proposed circuit is a microcontroller-based system, encompassing essential components including an **AND** gate device, a pair of MOSFETs, a step-up converter, a transformer, and several discrete elements such as an voltage rectifier, resistors, and capacitors. These components are classified into three blocks and applied within two distinct contexts, based on the differing transformers used in the amplification block. These contexts are denoted as the **"isolation transformer circuit"** and the **"audio transformer circuit"**.

While the command and conditioning blocks remain consistent across both approaches, the full operation of the circuit will be comprehensively detailed. This includes elucidating the operational characteristics of each amplification block in the context of the respective circuit configuration.

The circuit operates under the supervision of a microcontroller, specifically the ESP32. This microcontroller is responsible for generating pulse signals designed to function as stimulation pulses. In this particular context, the microcontroller employs PWM to create three controlled pulses: a modulator waveform (*IO25*), a positive pulse train (*IO32*), and a negative pulse train (*IO33*). These pulses are directed towards the conditioning block and are guided through **AND** gates. This setup allows the modulator pulse to determine the generation of stimulation pulses, influenced by its interaction with the positive and negative pulse trains.

By regulating the modulator pulse, the circuit manages the stimulation's frequency and pulse quantity. Additionally, the pulse trains, under the influence of PWM control, govern the pulse intensity. A detailed exploration of the software's attributes will be thoroughly presented in Chapter 5. Further on the conditioning block, the resulting positive and negative pulses are switched by an pair of N type MOSFETs model **30N06** (*Q1 & Q2*), and are direct the signals to the amplification block. The circuit schematic can be observed in Figure 3.5.

As mentioned previously, the distinguishing feature of the amplification block lies in the transformer model employed within each solution. In the initial approach, the Isolation transformer (VB 0.5/2/6) receives pulses from the conditioning block through the terminal pins of its low voltage side. Concurrently, the step-up converter supplies the requisite voltage to the

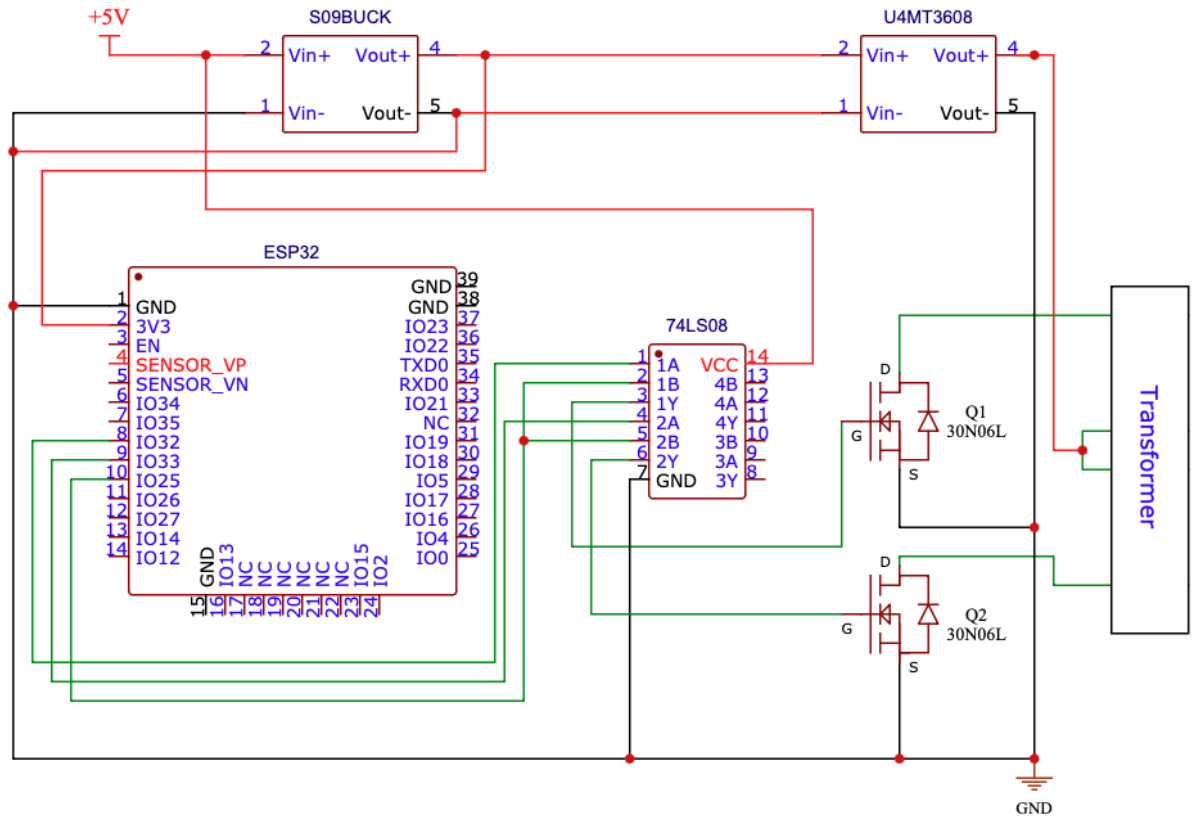

Figure 3.5: Circuit Schematic.

middle pins of the transformer, facilitating the amplification of the stimulation pulses. This procedural sequence enables the generation of biphasic stimulation pulses, characterized by the necessary intensity and waveform, essential for achieving effective electrical stimulation. A visual depiction of the Isolation transformer schematic is available in Figure 3.6.

The second approach, centered around the audio transformer MET-23, operates with a comparable rationale. However, due to the distinct pin configuration of this model, a pair of transformers is imperative to achieve the same objective. In this scenario, each transformer receives a pulse through one terminal of the low voltage side while being powered by the step-up converter through the other terminal. Consequently, it becomes feasible to generate the biphasic waveform by linking the high voltage side pins in parallel. Regarding this arrangement, the selection of the output connection was guided by its efficacy in producing the necessary output

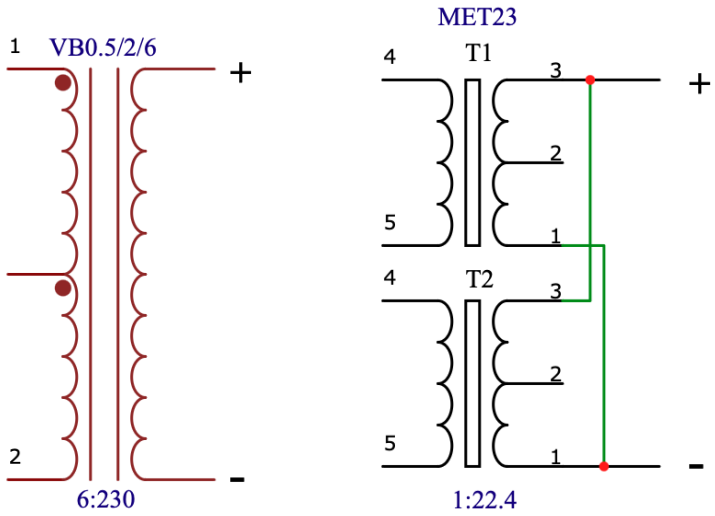

(a) Transformer VB 0.5/2/6 (b) Transformer MET-23

Figure 3.6: Transformers Schematic

waveform. In initial trials, the first approach involved a series connection of the transformer outputs. However, the parallel connection proved to yield superior overall outcomes. The resulting output waveform will be showcased in Chapter 5. A visual depiction of the Audio transformer schematic is available in Figure 3.6.

3.4 Circuit Implementation

Following the project's development timeline, after detailing the circuit description, the subsequent focus is on its implementation.

The development of the stimulation driver is intrinsically linked with its integration into the proposed solutions for the NanoStim and NanoID projects. The stimulation circuit is carefully devised to fulfill the requisite functions for both applications. In terms of prototype implementations, three distinct paths were pursued.

The initial approach, seen in the NanoStim prototype, represents an early model of the presented circuit. It is grounded in the concept of the Isolation Transformer, yet notable deviations in the conditioning block and software are evident. The second implementation, applied in the NanoID prototype, adheres closely to the previously described circuit design. Similarly, the

third prototype, constructed based on the Audio transformer circuit, strives to minimize the size and overall volume of the stimulation driver. Notably, considering the current circuit version, our discussion will exclusively focus on the second and third implementations.

The NanoID prototype is an application of Printed Circuit Board (PCB), consisting of four stimulation drivers based on the Isolation Transformer Circuit. Considering the project's demands, all functions are distributed across two microcontrollers. In this scenario, the stimulation drivers are paired off and allocated to each ESP32. This strategy is rooted in the microcontroller's processing capacity. Consequently, the system operates on the basis of an interaction between a master and slave microcontroller, where the mobile application assumes control over stimulation parameters.

This prototype incorporates several noteworthy attributes. It permits comprehensive management of stimulation pulses and facilitates stimulation activation through the implementation of a gyroscope. This gyroscope-based feature enables stimulation activation based on the patient's position, rendering it suitable for applications such as balance tests. When a specific threshold, as defined by the system calibration, is exceeded, stimulation is initiated. The NanoID prototype's features can be observed in Figure 3.7.

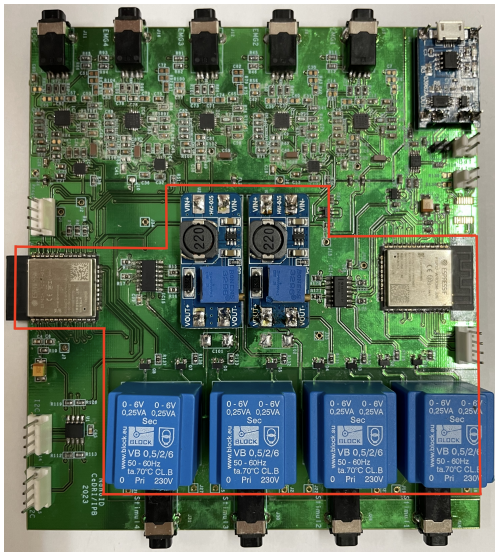

(a) Isolation Transformer Circuit

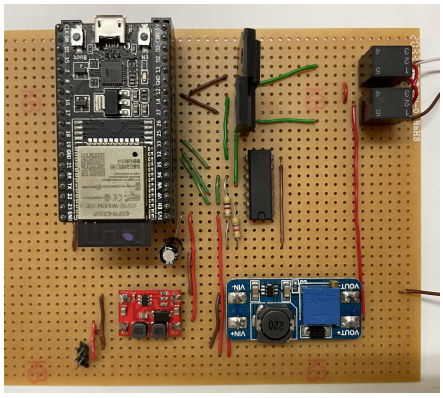

(b) Audio Transformer Circuit

Figure 3.7: Circuit Implementations

The Audio transformer circuit prototype is a single-driver circuit built on a prototype PCB as a proof of concept. Its purpose is to validate the audio transformer driver's performance while aiming to minimize the dimensions of the stimulation driver. Based on the audio transformer circuit, this prototype incorporates a single microcontroller responsible for communication and control, utilizing an application to define stimulation parameters.

Despite its exclusive focus on stimulation control through the application, this prototype can also accommodate the other functions introduced in the previous prototype. The Audio Transformer Prototype's characteristics are illustrated in Figure 3.7.

A comprehensive summary of the outcomes from both applications will be presented and described in Chapter 5.

Chapter 4

Software Development

This chapter aims the description and development of the system software that support the circuit applications. First the software architecture will be highlighted, and subsequently all the software features. Following the description, the code parts more relevant for the Stimulation driver operation will be explained in detail.

4.1 Architecture

The software architecture was designed to support a remote rehabilitation system integrated into a wearable device. This system was intended to provide a simple and user-friendly experience for both the patient and the healthcare professional responsible for the treatment. The software functions were developed by the NanoStim project as part of the biofeedback system. This section provides a brief overview of the software functions that underpin the system's operation.

The system's architecture was devised with the aim of fulfilling two primary functions. The first objective is the creation of a mobile application that enables the treatment to be administered at home, while also providing comprehensive control and system monitoring capabilities.

The second objective is to facilitate the transfer of all clinical data collected during the treatment session to the physiotherapist. In doing so, the healthcare professional can leverage this information to craft a personalized treatment plan tailored to the patient's condition.

All the data to be stored is highly sensitive, given its relevance to patient privacy. In recognition of this sensitivity, a series of security protocols have been implemented. These protocols are tailored to meet the minimum security requirements associated with the optimal application methods. The information storage is compartmentalized to prevent unauthorized access to sensitive data, effectively safeguarding it against potential cybernetic attacks.

In the context of this project, an overview of all software functions will be provided, with a particular focus on functions intricately tied to hardware operation, which will be elaborated upon in detail. Figure 4.1 illustrates the software architecture, offering an exemplification of all the functions to be examined.

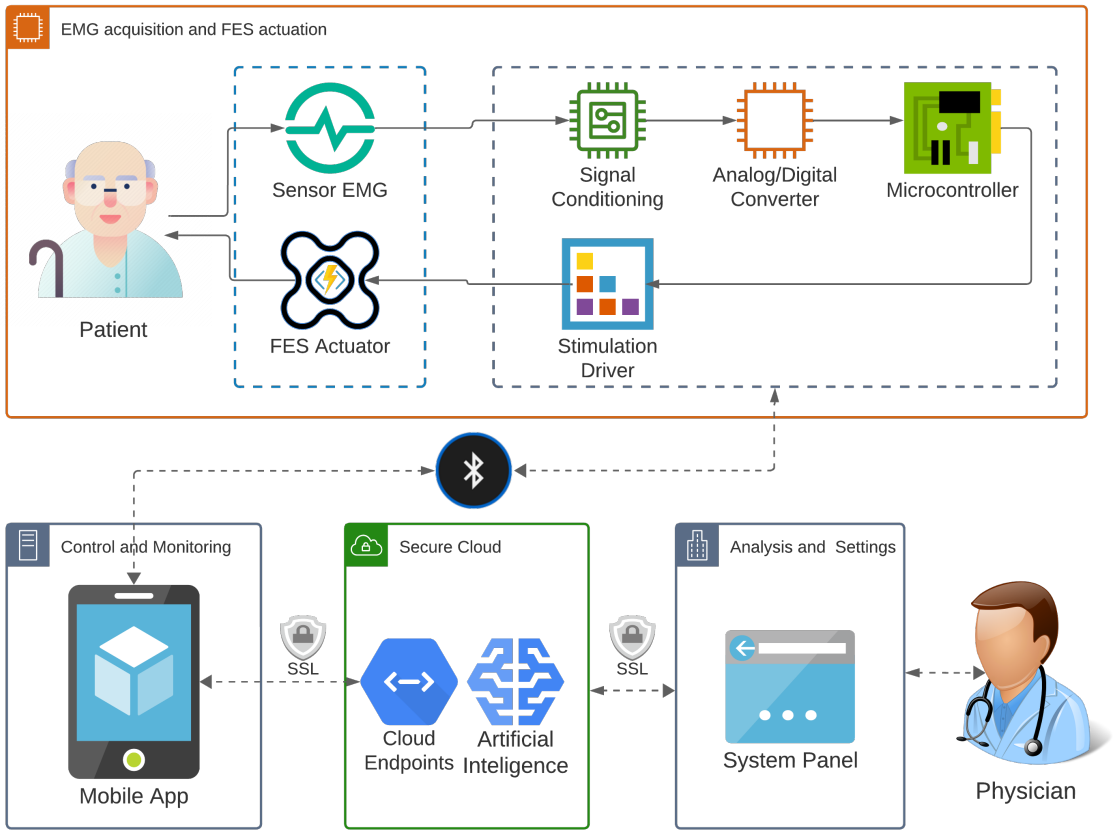

Figure 4.1: Software Architecture.

The presented design is based on a three-level architecture, using a smartphone as an intermediary device. In this context, the wearable represents the first layer, the mobile application

and system panel constitute the second layer, and the third layer pertains to the cloud functions.

The first layer refers to the Wearable system, which is composed of sensor data acquisition and the stimulation actuator. The wearable performs stimulation treatment and sends the collected data to the mobile application.

The second layer is composed of the mobile application and the system panel. The mobile application serves as an intermediary between the wearable and the cloud service. Its functions include receiving the stimulation protocol from the cloud and transmitting it to the wearable, organizing the data received from the wearable and sending it to the cloud, providing and collecting patient data, as well as controlling and monitoring the wearable system. The system panel serves as an administrative interface for professionals to manage patients and treatments. On this website, physiotherapists have access to the treatment plan, enabling them to visualize and adapt the electrical stimulation plan. Additionally, it is possible to access the acquired biofeedback data and communicate with the patients.

Finally, the third layer pertains to the cloud services. The cloud encompasses several functions, including the clinical service, management API, and Single Sign-On (SSO). The clinical service stores and processes all the clinical data used in a treatment, such as stimulation parameters and biofeedback collected by the wearable. The management API handles the necessary resources, such as patients, professionals, and messages, for the operation of the mobile app and system panel. Lastly, the SSO is responsible for generating access and refresh tokens to provide a single point of authentication, ensuring that access to all the services is secure. A detailed description of the architectural development within the project can be found at FRANCO *et. al.* [24].

Regarding the functioning of the stimulation driver, the software characteristics to be primarily explored are presented in the first layer, specifically in microcontroller programming. Therefore, later in this document, we will delve into the implementation of the electrical stimulation driver.

4.2 Implementation

In this section, will be present the implementation of the electrical stimulation software, emphasizing the specifics of pulse generation and control based on the proposed solution. Consequently, we will delve into a detailed discussion of the microcontroller's operation.

The electrical stimulation circuit is centered around an ESP32 microcontroller. In this context, the microcontroller takes on the responsibility of generating and controlling pulses in accordance with the parameters received from the mobile application. The ESP32 is programmed in **C++** using the Arduino Framework, establishing communication with the mobile app through a BLE connection. It generates the pulses using PWM based on a specific logic that has been developed to manage its parameters.

The software operates in two modes: the first involves direct control of stimulation parameters during a continuous stimulation session, while the second entails pre-setting the stimulation parameters to align with the treatment based on the movement data from the IMU. An illustration of this functionality is provided in Figure 4.2.

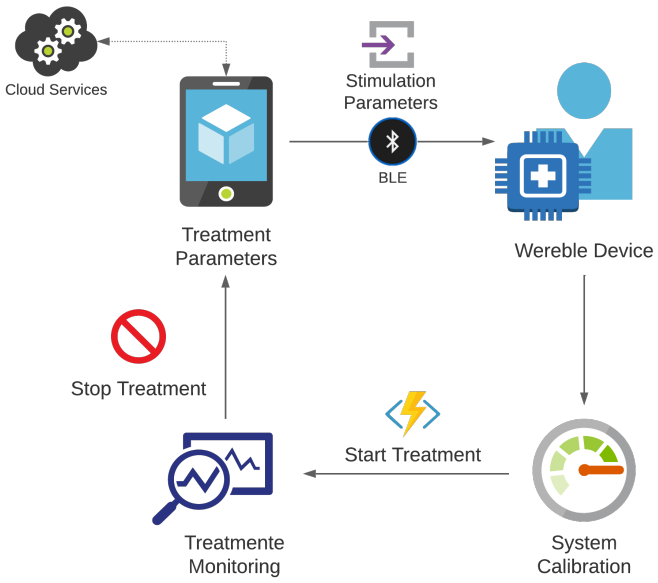

Figure 4.2: Stimulation setup example.

The electrical stimulation is controlled by adjusting three parameters: pulse frequency, pulse

duration, and the number of pulses. These parameters are regulated through PWM configured by the microcontroller, which receives information from the mobile app via BLE. The subsequent section will detail the PWM generation, its unique characteristics, and delve into the BLE functionality.

Bluetooth Low Energy Communication

BLE, as the name suggests, is a low-energy consumption communication protocol. The BLE protocol is a variant of the traditional Bluetooth protocol, and it exhibits several differences, including power consumption, range, throughput, and a few other characteristics.

Among these differences, the lower power consumption was the main factor that motivated the choice of this protocol. Even though BLE operates on the same frequency band as traditional Bluetooth, it consumes considerably less energy by remaining in a "sleep" state until a connection is initiated. This lower energy consumption characteristic allows BLE devices to operate for longer periods of time than traditional Bluetooth devices, as BLE only becomes active when a connections is established [25].

However, BLE has several limitations regarding data volume and packets. The Bluetooth version that includes Low Energy functionality starts at Bluetooth 4.0, which imposes a transmission data limit of 20 bytes per packet. Nevertheless, the ESP32 model utilized supports Bluetooth version 4.2, which allows for 517 bytes per packet [26].

Taking this factor into account, BLE is employed to enable the communication between the mobile application and the ESP32 microcontroller. In the context of this work, this communication is responsible for transmitting the stimulation parameters and receiving the stimulation logs generated during the treatment.

This protocol is employed in both the NanoStim and NanoID projects, but the way information is transmitted differs between them. In both projects, the parameters are sent in a packet containing a single vector. In the case of the NanoStim, this vector is composed of three values representing the stimulation parameters. On the other hand, in the NanoID, the vector consists of four values: the stimulation parameters, along with an "on/off" parameter to determine the state of the driver.

This way, the mobile application can send the necessary data for the microprocessor to generate the PWM pulses based on the required parameters.

PWM Configuration

Once the parameters are received from the application, the microcontroller generates the PWM pulses using the **LEDC** library, specifically designed for LED control and PWM generation. This library offers the capability to generate and control independent waveforms across eight channels, enabling functions such as generating three independent pulses or controlling LED intensities, for instance.

The LEDC channels are divided into two groups of eight: one group operates in high-speed mode, and the other operates in low-speed mode. The high-speed mode is implemented in hardware and offers automatic and glitch-proof changes of the PWM duty cycle. In contrast, the low-speed mode can be changed by the driver in software, although both modes can also be controlled through software adjustments.

Both of these groups of channels can utilize distinct clock sources. Furthermore, the PWM controller is capable of smoothly increasing or decreasing the duty cycle without any processor interference. This ensures that the generation of the PWM pulses does not interfere with the processing of other functions on the microcontroller, thus guaranteeing that the generation of the stimulation pulses does not disrupt other processes running on the microcontroller.

Considering this, the LEDC setup is achieved through three defined configuration steps. The first step involves Timer configuration, which specifies the PWM frequency and duty resolution. The second step is channel configuration, which associates the ESP32 General Purpose Input/Output (GPIO) and timer with the PWM signal output. The third step is PWM control, allowing for the software control of pulse duty cycle.

Following the PWM configuration steps, Algorithm 1 presents the code to perform the Timer configuration.

Algorithm 1 Timer Configuration

```
1 void configPWM(float frequency, int duty, int phase){
2     ledc_timer_config_t ledc_timer1 = {
3         .speed_mode = (ledc_mode_t) 0,
4         {.duty_resolution = LEDC_TIMER_10_BIT},
5         .timer_num = (ledc_timer_t) 0,
6         .freq_hz = frequency,
7     };
```

Listing 4.1 Timer Configuration

The initial setup begins with the configuration of the timers. This configuration is achieved by invoking the function **ledc_timer_config()**, whose structure is defined by **ledc_timer_config_t** (line 2). Within this structure, the library constants are defined, such as the speed mode, duty resolution, the timer to be used, and the PWM frequency.

This structure is named **ledc_timer1** (line 2) and will be invoked later in the code. Within the structure, the speed mode is set to high speed using the constant **ledc_mode_t** (line 3), and timer number "0" is assigned using the constant **ledc_timer_t** (line 5). The duty resolution is directly defined as 10 bits, following the library's convention, via the constant **LEDC_TIMER_10_BIT** (line 4). The frequency is determined by the parameter **frequency** (line 6), which is received from the function. It's worth noting that the duty and frequency are independent parameters, but they have an inversely proportional relationship; in other words, increasing the PWM frequency will result in a lower available duty resolution.

After configuring the timer, the next step is to set up the output channel. Channel configuration is performed using the function **ledc_channel_config()**. Similar to the timer configuration, this step requires the use of a structure. However, in this case, the structure is defined as **ledc_channel_config_t**, which encompasses all the channel configuration parameters. You can review the specific configuration details in Algorithm 2.

Similar to the timer configuration, the structure is defined as **ledc_channel1** (line 2) and will be called later by the function. Within this structure, the channel is defined, along with the associated GPIO, which in this case is specified as **STIMULATION_PIN_P** (line 3). The channel is configured using the constant **ledc_channel_t** with the value "0". Additionally, the

Algorithm 2 Channel Configuration

```
1
2  ledc_channel_config_t ledc_channel1 = {
3         .gpio_num       = STIMULATION_PIN_P,
4         .speed_mode     = (ledc_mode_t) 0,
5         .channel        = (ledc_channel_t) 0,
6         .intr_type      = (ledc_intr_type_t) LEDC_INTR_DISABLE,
7         .timer_sel      = (ledc_timer_t) 0,
8         .duty           = 0,
9         .hpoint         = 0
10     };
```

Listing 4.2 Channel Configuration

speed mode and timer selection are set based on the definitions from the timer configuration (lines 4 and 7), and PWM interruption is disabled using the constant **ledc_intr_type_t** (line 6), ensuring that control is handled entirely by software. Finally, the duty and phase values (lines 8 and 9) are both set to 0, as these values will be assigned by a function call later in the code. This channel configuration process is repeated three times throughout the code to configure all three PWM signals, as each one must have its channel configured.

The final step in the PWM configuration involves setting up the operation of the channels to generate the PWM signals and configuring the parameter changes to control them. You can observe this process in Algorithm 3.

Algorithm 3 Channel Configuration

```
1
2     ledc_timer_config(&ledc_timer1);
3     ledc_channel_config(&ledc_channel1);
4     ledc_channel_config(&ledc_channel2);
5     ledc_set_duty_with_hpoint((ledc_mode_t)0, (ledc_channel_t)0, duty,
    0);
6     ledc_set_duty_with_hpoint((ledc_mode_t)0, (ledc_channel_t)1, duty,
    phase);
7     ledc_update_duty((ledc_mode_t)0, (ledc_channel_t)0);
8     ledc_update_duty((ledc_mode_t)0, (ledc_channel_t)1);
```

Listing 4.3 PWM Control

In this step, the functions defined for the timer and channels are called (lines 2, 3, and 4), and the duty cycle is set and updated. The duty cycle is configured by invoking the function

ledc_set_duty_with_hpoint (lines 5 and 6), and this operation must be performed for each configured channel. This function retrieves various parameters previously defined, such as the timer's speed mode, the associated channel for each signal, as well as the duty and phase values. These parameters are then updated using the function **ledc_update_duty** (lines 7 and 8), which modifies the PWM parameters for the specified channels.

PWM Implementation

The PWM is configured to generate three signals: two pulse trains representing the positive and negative stimulation pulses, and one signal representing the carrier signal. In this context, the hardware selects the positive and negative pulses from the pulse trains based on the carrier signal, using an **AND** gate, as explained in Chapter 3.

Considering this, the PWM configuration must meet the requirements necessary to accomplish this task. In this context, for each stimulation driver, two timers need to be configured, along with three channels. One timer is allocated for the positive and negative pulse trains, and the other for the carrier signal, with one channel dedicated to each signal.

Following the implementation, the PWM pulses are generated and controlled based on three parameters transmitted from the mobile application to the microcontroller. These parameters are categorized into intensity, frequency, and the amount of pulses.

Regarding the circuit applications, the intensity and frequency are configured in a similar manner for both the **Isolation Transformer Circuit** and the **Audio Transformer Circuit**. The main difference lies in determining the number of pulses applied to each circuit's output and a minor distinction in the functioning of the pulse trains.

The frequency of the stimulation pulses is determined in a straightforward manner, based on the repetition of the carrier signal, which is configured as an absolute value. This results in the periodic repetition of the specified number of pulses at the output. In other words, the frequency corresponds to the rate at which the desired number of pulses is repeated per second.

Pulse intensity is determined by the duty cycle associated with the positive and negative pulse trains. The duty cycle of these pulses is defined in 512 bits, multiplied by two and distributed across two distinct phases. This configuration is necessary due to the phase distribution

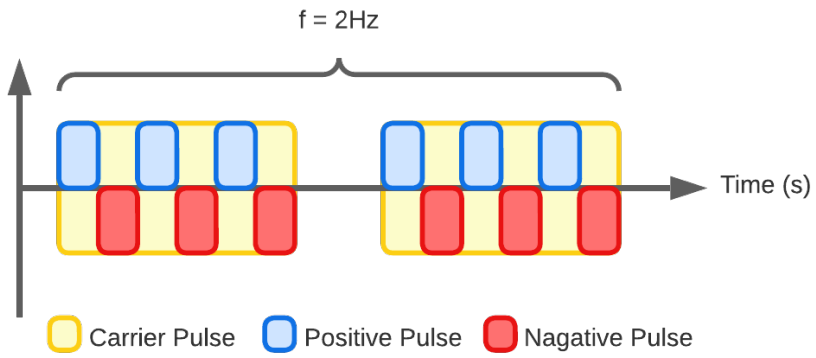

Figure 4.3: Frequency Example

of each pulse, as the positive and negative pulse trains commence at different times. Consequently, the duty cycle must be limited to a maximum value of 512 bits so that both phases can reach 1023 bits in accordance with the duty cycle resolution. This approach allows the generation of two equal signals to compose the biphasic waveform.

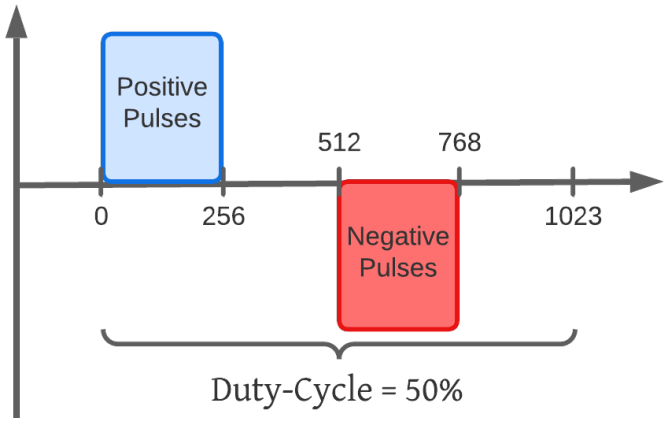

Figure 4.4: Duty-Cycle Example

The number of pulses is determined by how many pulses are "recruited" from the pulse trains by the carrier signal, achieved by altering the carrier time duration. This parameter represents the primary distinction between the two circuit applications. In the **Audio Transformer Circuit** application, the number of pulses is recruited by directly setting a specific time value, causing the pulses from the pulse trains to be directly applied to the output based on the carrier duration.

In contrast, the **Isolation Transformer Circuit** recruits the number of pulses while adhering

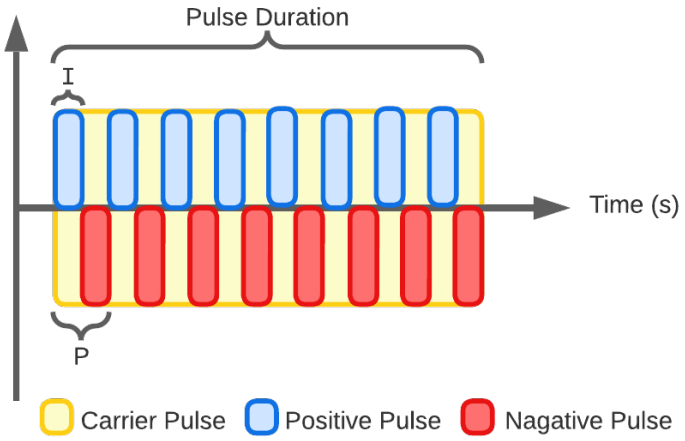

Figure 4.5: Audio transformer Pulse Duration

to a time rule. In this case, the carrier signal must align with the total period required for the desired number of pulses. This leads to a unique characteristic in this application, as the carrier signal is derived from the period value of the pulses in the pulse train. Consequently, the pulse trains must be disabled during the stimulation's downtime, which places additional processing demands on the microcontroller.

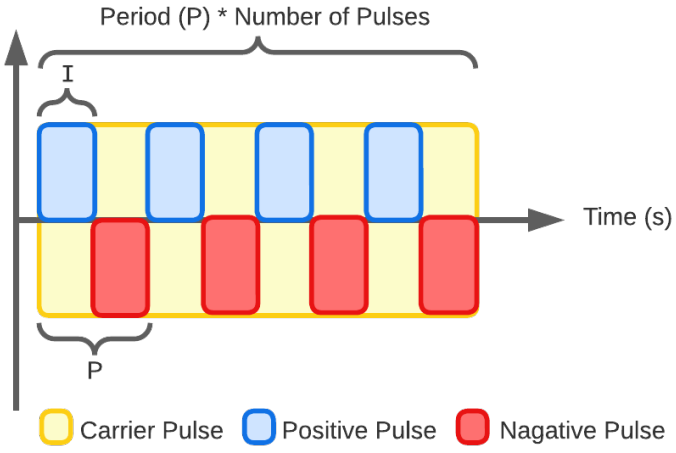

Figure 4.6: Isolation transformer Number of Pulses

The distinct approaches to determining the number of pulses are necessary to align with the frequency range of each transformer. The **Isolation Transformer**, which operates within a lower frequency range, is well-suited to the method of determining the number of pulses. On

the other hand, the **Audio Transformer** operates within a higher frequency range, necessitating the generation of a larger number of pulses to achieve the corresponding operational frequency of the component.

Chapter 5

Tests and Results

This chapter focuses on presenting the tests and evaluation of the proposed circuits. The tests were designed with the aim of validating each stimulation circuit and, consequently, providing sufficient data to facilitate a comparative analysis of both alternatives. The proposed tests are divided into two parts: the stimulation application on volunteers with lower limb involvement, and the application on volunteers with upper limb involvement.

The proposed test consists of presenting the overall functioning of each circuit alternative when applied to volunteers. The first test is performed on the subjects' lower limbs, specifically targeting the *vastus medialis* muscle located internally in the leg. The second test involves the application of stimulation pulses to an upper limb, specifically targeting the *Flexor Digitorum Profundus* muscle located in the forearm. The objective of these applications is to collect sufficient data to compare both circuits, considering both technical and practical attributes.

5.1 Tests

The tests will be divided into two parts, and both tests are designed to directly apply stimulation pulses for data collection. The first application test, referred to as the "Leg Validation Test", involves the application of electrical stimulation pulses to the *Vastus Medialis* muscle. The second validation test, named the "Arm Validation Test", will apply electrical stimulation to the forearm muscle, specifically the *Flexor Digitorum Profundus*. Both tests will be performed by

applying electrical stimulation using both the **Isolation Transformer Circuit** and the **Audio Transformer Circuit**. This approach allows us to verify their operation on distinct muscle groups.

The application tests received approval from the ethical committee of the Instituto Politécnico de Bragança (IPB) to conduct electrical stimulation for data acquisition for system evaluation and validation. As outlined in the provided document, volunteers will undergo the application of electrical stimulation pulses. These pulses do not pose a risk to the physical well-being of the subjects; however, they may cause discomfort or pain, depending on the applied stimulation parameters and the individual condition of each patient.

All tests were conducted on healthy subjects. The subjects had their information collected anonymously, with the only connection between the acquired data being their association with the stimulation parameters used to induce muscle contractions. Each volunteer received proper instructions regarding the test protocol and signed a consent form, thereby agreeing to participate in the tests.

5.1.1 Leg Validation Test

The objective of this test is to demonstrate the application and operation of both stimulation circuits on a leg muscle. These tests are conducted in the same manner for both circuits and involve incrementally adjusting the stimulation parameters until a visible muscle contraction is achieved. The pulses are applied to the *Vastus Medialis* muscle using commercially available wet electrodes. The test setup is illustrated in Figure 5.1.

The initial step of the tests involves positioning the electrodes on the muscle. Once the electrodes are securely in place, the first circuit to be tested is activated. In this instance, the **Isolation Transformer Circuit** is the first to undergo testing. Throughout the test, the intensity and the number of pulses are gradually increased. Intensity is progressively raised until a visible muscle contraction is observed, while the number of pulses is adjusted to ensure the volunteer's comfort. When a visible muscle contraction is achieved, the frequency is fine-tuned to maintain a consistent contraction rate, all while prioritizing the volunteer's comfort. The key parameters

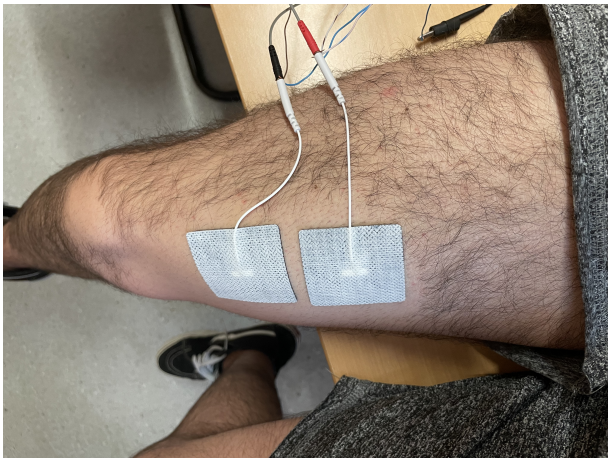

Figure 5.1: Electrodes positioning on the *Vastus Medialis* muscle

collected during this phase include the pulse intensity, measured at the pulse output in peak-to-peak Volts (V_{pk-pk}), the number of pulses, and the frequency determined by the application commands.

After completing this process, the test is repeated using the **Audio Transformer Circuit**. The protocol remains identical, with the only variation being the data collected. For the **Audio Transformer Circuit**, the parameter collected is the pulse duration value, as opposed to the number of pulses used in the **Isolation Transformer Circuit**. An example of the output pulses generated by both circuits during a muscle contraction can be seen in Figure 5.2.

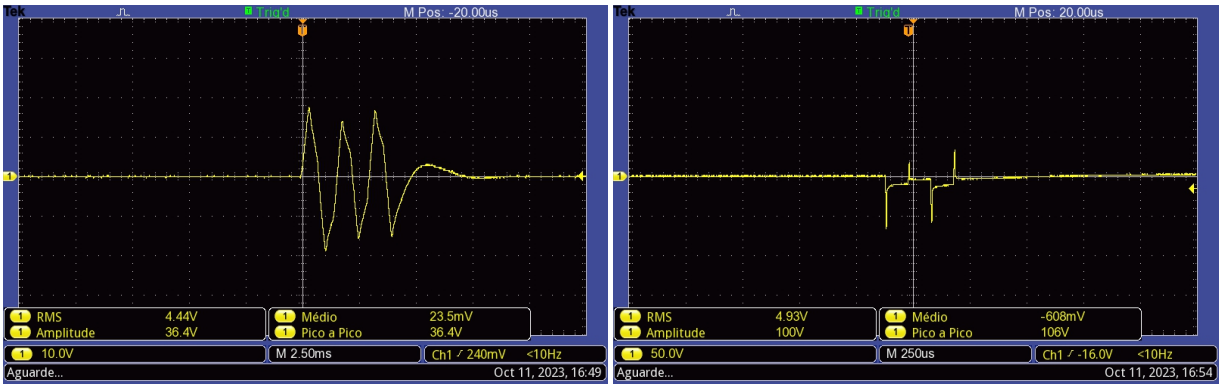

(a) Isolation Transformer Circuit output signal (b) Audio Transformer Circuit output signal

Figure 5.2: Output Stimulation pulses during a leg contraction.

After establishing the stimulation protocol, the circuit was tested on a group of volunteers.

Throughout the tests, both the physiological data of the volunteers and the resultant parameters from the muscle stimulation application were collected.

5.1.2 Arm Validation Test

Similar to the previous test, this one is focused on validating both circuits for the forearm muscle, specifically the *Flexor Digitorum Profundus*, which controls wrist movement. This test follows the same operational procedure: electrodes are placed on the targeted muscle, and the stimulation parameters are incrementally adjusted until a visible muscle contraction is observable. The stimulation pulses are delivered using wet commercial electrodes, and the test setup is depicted in Figure 5.3.

Figure 5.3: Electrodes positioning on the *Flexor Digitorum Profundus* muscle

The Arm validation tests were performed the same way as the tests performed on the Leg. The isolation transformer circuit was tested first, the stimulation parameter were incremented respecting the volunteer comfort, until the muscle contraction could be observed. This protocol was repeated with the Audio transformer circuit. In both applications the stimulation parameters are collected as the muscle reach a constant contraction point. The parameter collected are the same, Voltage(V) peak-to-peak, frequency, number of pulses (Isolation transformer circuit) and pulse duration (Audio transformer circuit). An example of output pulses from the circuits con be observed in Figure 5.4

The Arm validation tests were conducted in the same manner as the tests performed on the Leg. Initially, the isolation transformer circuit was tested, and stimulation parameters were gradually increased while considering the volunteer's comfort until a visible muscle contraction was achieved. This protocol was subsequently repeated with the Audio transformer circuit. In both applications, the stimulation parameters were recorded when the muscle reached a consistent contraction point. The parameters collected are consistent and include Voltage peak-to-peak (V_{pk-pk}), frequency, number of pulses (for the Isolation transformer circuit), and pulse duration (for the Audio transformer circuit). An illustration of the output pulses generated by the circuits can be observed in Figure 5.4.

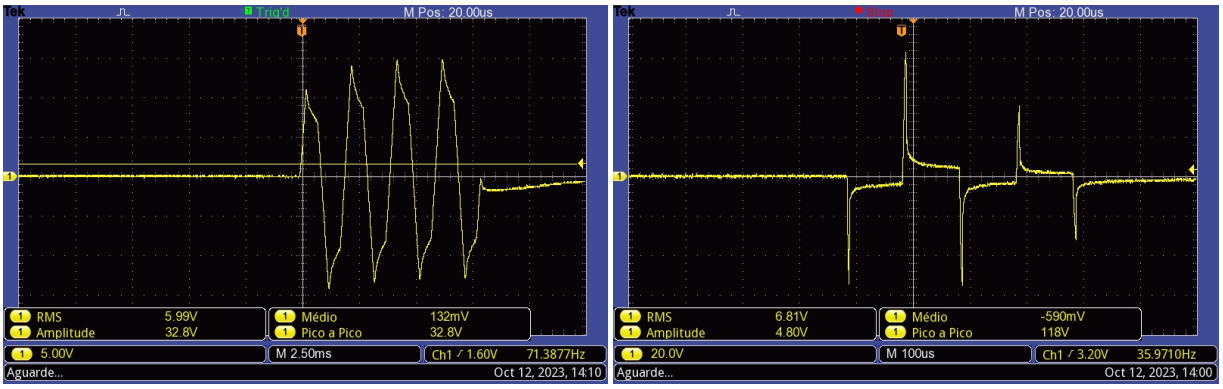

(a) Isolation Transformer Circuit output signal (b) Audio Transformer Circuit output signal

Figure 5.4: Output Stimulation pulses during a contraction on the forearm.

The Arm validation tests were conducted using the same group of volunteers as the Leg validation tests. The data collected from the circuit operation was consistent across both sets of tests.

5.2 Results and Evaluation

This section will present the results collected from the tests, discuss and analyze the data obtained from the applications of both circuits, and compare their overall performance. The results will be presented in several parts. Firstly, the profiles of the volunteers and the averages of their physiological information will be presented, with the aim of analyzing the population involved

in the tests and the test procedures. Secondly, the stimulation values will be presented and discussed to emphasize the performance of both circuits on different physiology's. Lastly, a comfort evaluation analysis will be conducted based on the feedback received from the volunteers after undergoing tests with both circuits.

5.2.1 Volunteers Profile Analysis

In total, the tests were conducted on ten volunteers, with an equal gender distribution of five men and five women. All volunteers are young adults, in good health, without chronic health issues, and they are all associated with the academic environment, either as students or researchers.

All the volunteers underwent the same test protocols. The test procedures and setups were identical for all volunteers. Firstly, the study's objectives were explained, emphasizing the significance of these tests for the study. Secondly, the test protocols were comprehensively outlined, with particular attention given to the explanation of electrode placement and a description of the overall sensation of the stimulation. Throughout the tests, volunteers were continuously monitored to prevent any discomfort or pain resulting from parameter changes. It is important to note that no volunteer reported any pain or discomfort during the stimulation process in either circuit application.

Volunteers Characteristics

The ten volunteers provided their information, including gender, age, height, and weight. This information was used to calculate the BMI. In this case, this measurement method was exclusively applied to differentiate between various characteristics of the volunteers, making it easier to identify differences in their physical constitution. Additionally, a comfort level assessment was conducted based on the volunteers' experiences, which will be further explored in this chapter. The collected data was categorized by gender, while other characteristics had their mean and standard deviation calculated to facilitate data analysis without compromising the confidentiality of the volunteers' information. The collected information is presented in Table 5.1.

Gender	Age	Height (m)	Weight (kg)	BMI (kg/m^2)
Man	25.20 ($\pm$ 1.47)	1.75 ($\pm$ 0.07)	80.27 ($\pm$ 12.34)	27.00 ($\pm$ 6.00)
Woman	27.00 ($\pm$ 2.35)	1.61 ($\pm$ 0,03)	67.31 ($\pm$ 16.78)	26.00 ($\pm$ 6.00)

Table 5.1: Mean $\pm$ standard deviation of the volunteers physical data.

Concerning the collected data, it is evident that the volunteer population exhibits a diverse range of physical characteristics. By examining the mean values of the BMI, calculated as the body mass divided by the square of the height, it becomes apparent that there is a wide distribution of body types. This diversity provides a valuable range of scenarios for the applications of both circuits, enabling the tests to encompass a broad spectrum of physical conditions.

It's important to emphasize that this study does not make any value judgments regarding the physical constitution of any volunteer. This information is solely used to assess the potential applications of each proposed solution.

5.2.2 Electrical Stimulation Results

The ES results primarily consist of the recorded values of the output signal during the stimulation test protocol. These values correspond to the point at which a muscle contraction was observed during the test applications. In this context, the parameters associated with the output intensity of the stimulation signal, as well as the peak-to-peak Voltage from the stimulation signal acquired during the muscle contraction, were collected. The results will be presented based on the type of circuit and test protocol.

Isolation Transformer Circuit

The command values associated with the Isolation transformer circuit are measured in microseconds (μs), and the output intensity is measured in Volts peak-to-peak (V_{pk-pk}). For the purpose of data analysis, the values will be presented as the mean and standard deviation of the stimulation values for each test. The results of the Isolation Transformer Circuit for both test applications can be found in Table 5.2.

Test Protocol	Pulse Duration (μs)	Tension (V_{pk-pk})
Arm Test	481.00 ($\pm$ 124.00)	37.88 ($\pm$ 12.54)
Leg Test	549.60 ($\pm$ 144.00)	49.16 ($\pm$ 12.53)

Table 5.2: Mean $\pm$ standard deviation of the Isolation Transformer Circuit stimulation results.

These values represent the required intensity levels to induce muscle stimulation in the volunteers. In general, the voltage required to elicit a contraction in the arm muscle is lower than the voltage needed to stimulate the leg muscle. This difference can be attributed to the contrasting sizes of the two muscle groups. For a more in-depth analysis, Figure 5.5 presents a graph comparing the stimulation values to the BMI of the volunteers.

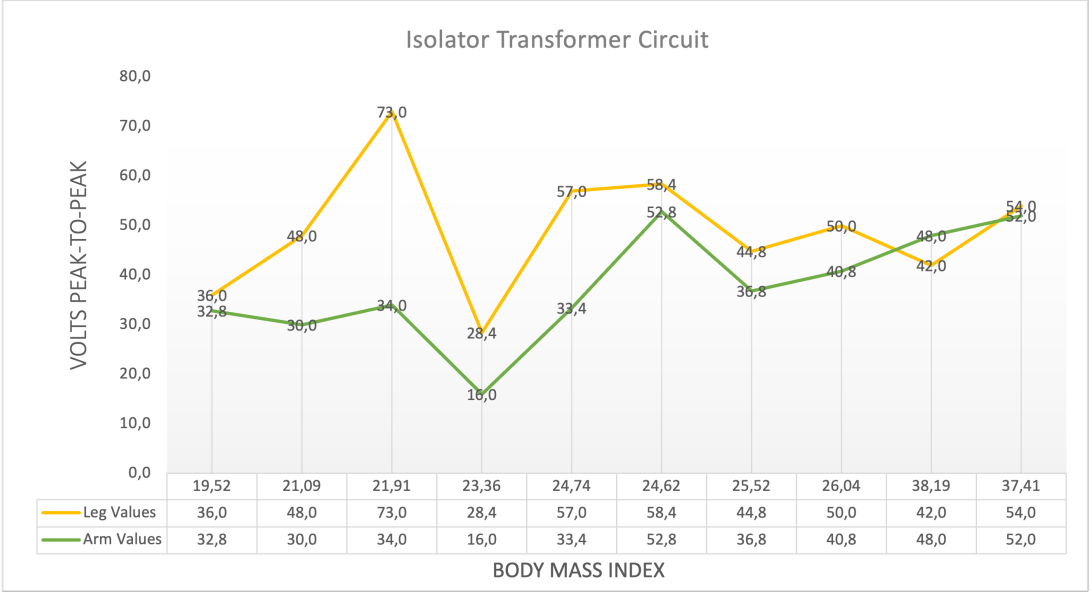

Figure 5.5: Stimulation voltage related to the BMI values of the volunteers

The graph presents the peak-to-peak voltage value on the Y-axis and the BMI measurement on the X-axis, expressed in kg/m^2. The yellow line represents the required voltage to induce a muscle contraction in the leg, and the green line represents the required voltage for an arm muscle contraction. It can be observed that in most cases, the stimulation value is proportional to the body mass value. However, there are exceptions. For instance, individuals who engage in regular physical exercise generally require less intensity to generate a muscle contraction due to a more developed muscular constitution. On the other hand, difficulties in achieving

stimulation may arise due to the accumulation of body fat in the stimulation area. Another noteworthy point is the deviation of *73V* in the leg value, which can occur if the electrodes responsible for applying the stimulation are poorly positioned. This situation is more likely to occur if the target muscle for stimulation is relatively small. In summary, the **Isolation Transformer Circuit** successfully induced muscle contractions in all volunteers during the Arm Test protocol. However, during the Leg Test protocol, the circuit was effective in inducing muscle contractions in nine out of ten volunteers.

Audio Transformer Circuit

For the Audio Transformer Circuit, the command values are set in duty-cycle bits, and the output voltage is measured in Volts peak-to-peak (V_{pk-pk}). The command values of this circuit will also be presented as the mean and standard deviation of the stimulation values for each test. The results for the Audio Transformer Circuit in both stimulation tests can be found in Table 5.3.

Test Protocol	Level (bits)	Tension (V_{pk-pk})
Arm Test	35.00 ($\pm$ 10.00)	100,40 ($\pm$ 21.79)
Leg Test	41.00 ($\pm$ 20.00)	126.20 ($\pm$ 17.44)

Table 5.3: Mean $\pm$ standard deviation of the Audio Transformer Circuit stimulation results.

The stimulation values obtained during the tests with the Audio Transformer Circuit differ significantly from those collected in the previous circuit, owing to differences in their operation. In this case, the values vary around 100 volts, and the mean of the command level fluctuates within a narrower range, allowing this circuit to achieve a wide range of output intensity with relatively small command changes. For a deeper analysis of the acquired data, Figure 5.6 illustrates the stimulation values in relation to the BMI data of the volunteers.

Similar to the previous graph, the Y-axis represents the Voltage peak-to-peak (V_{pk-pk}) values, and the X-axis displays the BMI values of the volunteers measured in kg/m^2. In this graph, the orange line represents the stimulation values acquired during the Leg Test protocol, and the gray line represents the stimulation values acquired during the Arm Test protocol. Overall,

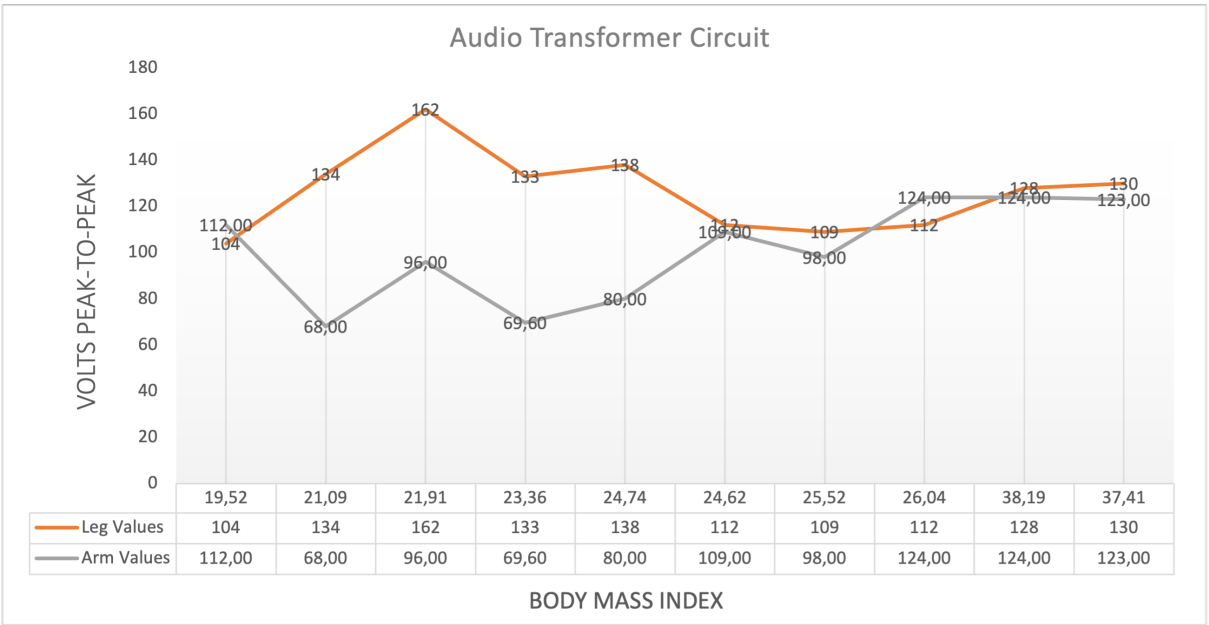

Figure 5.6: Stimulation voltage related to the BMI values of the volunteers

in this application, the voltage required to stimulate the Arm muscle is lower than the voltage needed to stimulate the Leg muscle due to their size difference. However, it is noticeable that in half of the cases (6 out of 10), the stimulation values to generate contractions in the Arm and Leg muscles are similar. Concerning the four distinct values, it's evident that the increase in stimulation values is not necessarily correlated with the individual's body mass. This deviation could be attributed to the accumulation of body fat in the area. Despite the observed deviations, the **Audio Transformer Circuit** successfully induced muscle contractions in all volunteers during both test protocols.

5.2.3 Comfort Analysis

The comfort analysis involved questioning the volunteers regarding their comfort levels during the electrical stimulation applications of both circuits in the tests. This assessment utilized a scale ranging from one to ten, where one represented significant discomfort or pain, and ten represented an experience closest to a voluntary contraction. The data was categorized by circuit and test application. The comfort evaluations are presented in Figure 5.7.

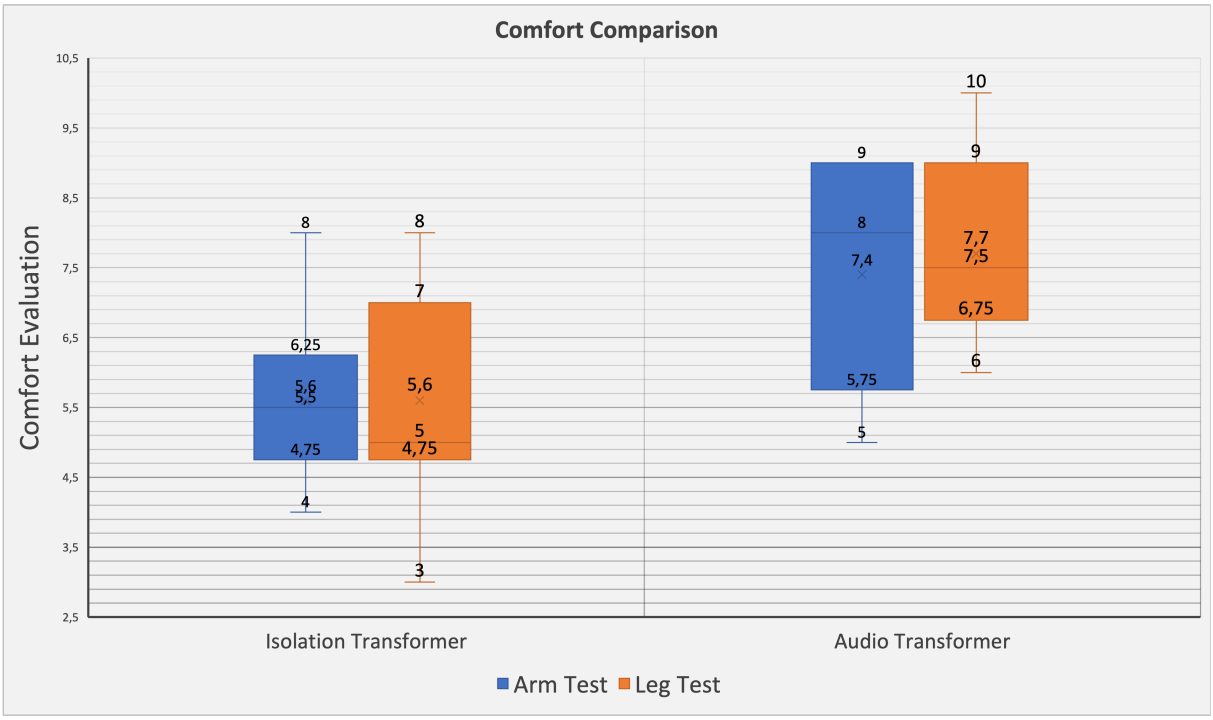

Figure 5.7: Comfort valuation comparison between both circuits applications.

This graph illustrates a comparison of comfort ratings provided by volunteers after completing tests with both circuits. The Arm tests are depicted in blue, and the Leg tests are shown in orange. Upon reviewing the presented data, it is evident that following the Arm tests, the mean comfort evaluation is 5.6 for the Isolation Transformer and 7.4 for the Audio Transformer. The highest comfort rating for the Isolation Transformer circuit was 8, while the lowest was 4. For the Audio Transformer circuit, the highest rating was 10, and the lowest was 5. Regarding the evaluation results after the Leg tests, the mean comfort rating is 5.6 for the Isolation Transformer and 7.7 for the Audio Transformer. The highest comfort rating for the Isolation Transformer was 8, with the lowest being 3, while for the Audio Transformer, the highest rating was 10, and the lowest was 6.

Based on the evaluation data gathered from the tests, it is possible to infer that the Audio Transformer Circuit was better received in terms of stimulation comfort by the volunteers when compared to the Isolation Transformer Circuit. Consequently, as per the feedback from the volunteers, the Audio Transformer Circuit offers a higher level of comfort during the application

of stimulation pulses.

5.2.4 Evaluation

Taking into account all the presented results, both circuits operate in significantly distinct ways. The overall intensity required to achieve stimulation varies across the circuits due to differences in their control methods. To recap the test results, the **Isolation Transformer Circuit** successfully induced muscle contractions in all volunteers during the Arm Test protocol and in 9 out of 10 volunteers during the Leg Test protocol. On the other hand, the **Audio Transformer Circuit** managed to induce muscle contractions in all volunteers during both test protocols. In terms of comfort evaluation, the feedback from the volunteers favored the **Audio Transformer Circuit**, as indicated by the higher mean values in both test evaluations. This suggests that the Audio Transformer circuit is more comfortable.

Taking into account the range of applications and comfort as the decisive factors, the **Audio Transformer Circuit** emerges as the superior choice for implementation on the wearable systems.

Chapter 6

Conclusions

This project was undertaken with the aim of creating a FES driver to complement a wearable physiotherapy system. The goal was to propose and design a circuit capable of generating muscle contractions while adhering to the system's constraints. In other words, the objective was to develop a compact circuit with limited processing power that could induce muscle contractions across a broad spectrum of diverse applications.

The development of the stimulation driver led to the creation of two transformer-based circuit alternatives aimed at achieving the desired stimulation outcomes. Each alternative is based on a specific type of transformer, and the method of stimulation control is adapted to the operational characteristics of each model. These alternatives were named the **Isolation Transformer Circuit** and the **Audio Transformer Circuit**. In both cases, an ESP32 microcontroller is responsible for overall control, and the pulses are generated through PWM controlled by a mobile application. These solutions enabled the generation and control of stimulation pulses in accordance with the underlying physiological principles.

The applications of both circuits led to the generation of muscle contractions in accordance with the parameters set by the mobile application. In the validation tests of both circuits, stimulation pulses were applied to ten volunteers in two distinct muscle groups, one in the leg and one in the forearm. The collected results demonstrate that during the leg test protocol, the Isolation Transformer Circuit managed to stimulate 9 out of 10 volunteers, while the Audio Transformer Circuit successfully stimulated all the volunteers. During the arm test protocol, both circuits

successfully stimulated all the volunteers.

In addition to the validation tests, a comfort evaluation was conducted after the test applications, where all volunteers assessed the comfort levels of the circuit applications. The overall result of the evaluation showed that, for both test protocols, the **Audio Transformer Circuit** delivered electrical stimulation with greater comfort. In light of the results presented and the evaluation based on the collected data, it is evident that the **Audio Transformer Circuit** stands out as the superior option among the two alternatives presented.

Taking into account all the factors presented, it is feasible to conclude that this work successfully developed two fully functional and controllable FES circuits that adhere to the physiological principles for inducing muscle contractions through the application of electrical pulses. Furthermore, the application of these circuits was demonstrated on a diverse range of volunteers, and based on the collected data, the optimal circuit option for integration into the wearable system can be determined.

As future work related to this topic, it is advisable to explore a more compact solution for pulse amplification, further reducing the size of the stimulation driver and, consequently, the wearable device. In addition to electronic developments, it would be beneficial to devise an intelligent method for adjusting the stimulation parameters. Currently, these adjustments are made through a mobile application, but the next step may involve the implementation of rule-based parameter changes using machine learning or artificial intelligence techniques.

Bibliography

[1] C. L. LYNCH and M. R. POPOVIC, "Functional electrical stimulation," *IEEE Control Systems Magazine*, vol. 28, no. 2, pp. 40–50, 2008. DOI: 10.1109/MCS.2007.914689.

[2] A. Masdar, B. K. K. Ibrahim, and M. M. Abdul Jamil, "Development of wireless-based low-cost current controlled stimulator for patients with spinal cord injuries," in *2012 IEEE-EMBS Conference on Biomedical Engineering and Sciences*, 2012, pp. 493–498. DOI: 10.1109/IECBES.2012.6498175.

[3] H. Wang, G. Guan, Q. He, *et al.*, "An electrical muscle simulator based on functional electrical stimulation," in *2012 IEEE International Conference on Robotics and Biomimetics (ROBIO)*, 2012, pp. 1906–1911. DOI: 10.1109/ROBIO.2012.6491246.

[4] T. Franco, L. Sestrem, P. R. Henriques, *et al.*, "Motion sensors for knee angle recognition in muscle rehabilitation solutions," *Sensors*, vol. 22, no. 19, p. 7605, 2022.

[5] P. H. Peckham and J. S. Knutson, "Functional electrical stimulation for neuromuscular applications," *Annual Review of Biomedical Engineering*, vol. 7, no. 1, pp. 327–360, 2005, PMID: 16004574. DOI: 10.1146/annurev.bioeng.6.040803.140103. eprint: https://doi.org/10.1146/annurev.bioeng.6.040803.140103. [Online]. Available: https://doi.org/10.1146/annurev.bioeng.6.040803.140103.

[6] A. M. Stewart, C. G. Pretty, and X. Chen, "Design and testing of a novel, low-cost, low-voltage, functional electrical stimulator," in *2016 12th IEEE/ASME International Conference on Mechatronic and Embedded Systems and Applications (MESA)*, 2016, pp. 1–6. DOI: 10.1109/MESA.2016.7587155.

[7] D. B. Popović, "Advances in functional electrical stimulation (fes)," *Journal of Electromyography and Kinesiology*, vol. 24, no. 6, pp. 795–802, 2014, ISSN: 1050-6411. DOI: https://doi.org/10.1016/j.jelekin.2014.09.008. [Online]. Available: https://www.sciencedirect.com/science/article/pii/S1050641114001953.

[8] J. Burridge, M. Haugland, B. T. Larsen, *et al.*, "Phase ii trial to evaluate the actigait implanted drop-foot stimulator in established hemiplegia," *Journal of rehabilitation medicine*, vol. 39, no. 3, pp. 212–218, 2007.

[9] D. G. Everaert, R. B. Stein, G. M. Abrams, *et al.*, "Effect of a foot-drop stimulator and ankle–foot orthosis on walking performance after stroke: A multicenter randomized controlled trial," *Neurorehabilitation and neural repair*, vol. 27, no. 7, pp. 579–591, 2013.

[10] M. R. Popovic, T. A. Thrasher, V. Zivanovic, J. Takaki, and V. Hajek, "Neuroprosthesis for retraining reaching and grasping functions in severe hemiplegic patients," *Neuromodulation: Technology at the Neural Interface*, vol. 8, no. 1, pp. 58–72, 2005.

[11] R. Nataraj, M. L. Audu, and R. J. Triolo, "Comparing joint kinematics and center of mass acceleration as feedback for control of standing balance by functional neuromuscular stimulation," *Journal of neuroengineering and rehabilitation*, vol. 9, pp. 1–11, 2012.

[12] A. Dutta, R. Kobetic, and R. J. Triolo, "An objective method for selecting command sources for myoelectrically triggered lower-limb neuroprostheses," *J Rehabil Res Dev*, vol. 48, no. 8, pp. 935–948, 2011.

[13] B. M. Doucet, A. Lam, and L. Griffin, "Neuromuscular electrical stimulation for skeletal muscle function," *The Yale journal of biology and medicine*, vol. 85, no. 2, p. 201, 2012.

[14] D. M. Durand, W. M. Grill, and R. Kirsch, "Electrical stimulation of the neuromuscular system," *Neural engineering*, pp. 157–191, 2005.

[15] D. Rushton, "Functional electrical stimulation," *Physiological measurement*, vol. 18, no. 4, p. 241, 1997.

[16] K. Cheng, Y. Lu, K.-Y. Tong, A. Rad, D. Chow, and D. Sutanto, "Development of a circuit for functional electrical stimulation," *IEEE Transactions on Neural Systems and Rehabilitation Engineering*, vol. 12, no. 1, pp. 43–47, 2004. DOI: 10.1109/TNSRE.2003.819936.

[17] J. Velloso and M. Souza, "A programmable system of functional electrical stimulation (fes)," in *2007 29th Annual International Conference of the IEEE Engineering in Medicine and Biology Society*, 2007, pp. 2234–2237. DOI: 10.1109/IEMBS.2007.4352769.

[18] M. Chen, B. Wu, X. Lou, *et al.*, "A self-adaptive foot-drop corrector using functional electrical stimulation (fes) modulated by tibialis anterior electromyography (emg) dataset," *Medical Engineering Physics*, vol. 35, no. 2, pp. 195–204, 2013, ISSN: 1350-4533. DOI: https://doi.org/10.1016/j.medengphy.2012.04.016. [Online]. Available: https://www.sciencedirect.com/science/article/pii/S1350453312001026.

[19] H.-P. Wang, Z.-G. Wang, X.-Y. Lü, Z.-H. Huang, and Y.-X. Zhou, "Design of a pulse-triggered four-channel functional electrical stimulator using complementary current source and time division multiplexing output method," in *2015 37th Annual International Conference of the IEEE Engineering in Medicine and Biology Society (EMBC)*, 2015, pp. 1671–1674. DOI: 10.1109/EMBC.2015.7318697.

[20] R. Shirafkan, O. Shoaei, and M. K. Ahmadi, "A high efficient adiabatic transcutaneous electrical nerve stimulator (tens) with current regulation," *AEU - International Journal of Electronics and Communications*, vol. 123, p. 153 275, 2020, ISSN: 1434-8411. DOI: https://doi.org/10.1016/j.aeue.2020.153275. [Online]. Available: https://www.sciencedirect.com/science/article/pii/S1434841120307366.

[21] B. Basumatary, R. S. Halder, and A. Sahani, "A microcontroller based charge balanced trapezoidal stimulus generator for fes system," in *2021 IEEE International Instrumentation and Measurement Technology Conference (I2MTC)*, 2021, pp. 1–4. DOI: 10.1109/I2MTC50364.2021.9459837.

[22] M. C. Santos, G. Bedenik, S. Carvalho, *et al.*, "Easy-to-implement configurable multimodal electrostimulator," in *2021 5th International Symposium on Instrumentation Systems, Circuits and Transducers (INSCIT)*, 2021, pp. 1–6. DOI: 10.1109/INSCIT49950.2021.9557252.

[23] T. F. De Almeida, L. H. B. Borges, and A. F. O. d. A. Dantas, "Development of an iot electrostimulator with closed-loop control," *Sensors*, vol. 22, no. 9, p. 3551, 2022.

[24] T. Franco, P. R. Henriques, P. Alves, *et al.*, "System architecture for home muscle rehabilitation treatment," in *World Conference on Information Systems and Technologies*, Springer, 2022, pp. 305–315.

[25] Litum. "What is bluetooth low energy (ble)? how does ble work?" (), [Online]. Available: https://litum.com/what-is-ble-how-does-ble-work/. (accessed: 18.09.2023).

[26] T. Franco, P. R. Henriques, P. Alves, *et al.*, "Myhealth: A mobile app for home muscle rehabilitation," in *2022 IEEE 10th International Conference on Serious Games and Applications for Health(SeGAH)*, 2022, pp. 1–7. DOI: 10.1109/SEGAH54908.2022.9978561.

Appendix A

ESP32 Codes

This appendix presents the codes applied to control both transformers circuits.

A.1 Isolation Transformer Circuit Code

```
1
2  #include <Arduino.h>
3  #include "stimulation.hpp"
4  #include <driver/ledc.h>
5  #include "config_pins.h"
6  #include "global_var.hpp"
7  #include "Wire.h"
8
9  #define STIMULATION_ENABLE_1 32 // Generic GPIO definition
10 #define STIMULATION_PIN_P_1 33
11 #define STIMULATION_PIN_N_1 25
12
13 void configPWM(float frequency, int duty, int phase, float
       masterfrequency, int masterduty){
14
15         ledc_timer_config_t ledc_timer1 = {   /*Positive and negative
       ulses timer configuration*/
16         .speed_mode = (ledc_mode_t) 0,
```

```
17        {.duty_resolution = LEDC_TIMER_10_BIT},
18        .timer_num = (ledc_timer_t) 0,
19        .freq_hz = frequency,
20        };
21
22
23        ledc_timer_config_t ledc_timer3 = {   /*Modulator pulse timer
    configuration*/
24        .speed_mode = (ledc_mode_t) 0,
25        {.duty_resolution = LEDC_TIMER_10_BIT},
26        .timer_num = (ledc_timer_t) 1,
27        .freq_hz = masterfrequency,
28        };
29
30
31        ledc_channel_config_t ledc_channel1 = {
32        .gpio_num       = STIMULATION_PIN_N_1,  /*Negative pulse channel
     configuration*/
33        .speed_mode     = (ledc_mode_t) 0,
34        .channel        = (ledc_channel_t) 0,
35        .intr_type      = (ledc_intr_type_t) LEDC_INTR_DISABLE,
36        .timer_sel      = (ledc_timer_t) 0,
37        .duty           = 0,
38        .hpoint         = 0
39        };
40
41        ledc_channel_config_t ledc_channel2 = { /*Positive pulse channel
     configuration*/
42        .gpio_num       = STIMULATION_PIN_P_1,
43        .speed_mode     = (ledc_mode_t) 0,
44        .channel        = (ledc_channel_t) 1,
45        .intr_type      = (ledc_intr_type_t) LEDC_INTR_DISABLE,
46        .timer_sel      = (ledc_timer_t) 0,
47        .duty           = 0,
48        .hpoint         = 0
```

```
49        };
50
51        ledc_channel_config_t ledc_channel5 = { /*Modulator pulse
    channel configuration*/
52        .gpio_num       = STIMULATION_ENABLE_1,
53        .speed_mode     = (ledc_mode_t) 0,
54        .channel        = (ledc_channel_t) 2,
55        .intr_type      = (ledc_intr_type_t) LEDC_INTR_DISABLE,
56        .timer_sel      = (ledc_timer_t) 1,
57        .duty           = 0,
58        .hpoint         = 0
59        };
60
61
62        /*Functions call*/
63
64        ledc_timer_config(&ledc_timer1);
65        ledc_channel_config(&ledc_channel1);
66        ledc_channel_config(&ledc_channel2);
67        ledc_set_duty_with_hpoint((ledc_mode_t)0, (ledc_channel_t)0,
    duty, 0);
68        ledc_set_duty_with_hpoint((ledc_mode_t)0, (ledc_channel_t)1,
    duty, phase);
69        ledc_update_duty((ledc_mode_t)0, (ledc_channel_t)0);
70        ledc_update_duty((ledc_mode_t)0, (ledc_channel_t)1);
71
72        ledc_timer_config(&ledc_timer3);
73        ledc_channel_config(&ledc_channel5);
74        ledc_set_duty_with_hpoint((ledc_mode_t)0, (ledc_channel_t)2,
    masterduty, 0);
75        ledc_update_duty((ledc_mode_t)0, (ledc_channel_t)2);
76     }
77
78     void stimulation(int I, int P, int F)
79 {
```

```
80      Serial.print("Stimulation intensity: ");
81      Serial.println(I);
82
83      int R = 0;
84
85      period[enable] = ((I * 4));
86      frequency[enable] = 1/(period[enable]/1000000);
87      step[enable] = period[enable]/1023; // 10 bits of resolution
88      duty[enable] = I / step[enable]; // us to duty cycle
89      shift[enable] = 511; // pulse shift
90
91      masterintensity[enable] = period[enable]*P;
92
93
94      masterfrequency[enable] = F;    // 1/(masterperiod[enable]/1000000);
95
96      masterperiod[enable] = 1/((float)F/1000000);
97      masterstep[enable] = (float)masterperiod[enable]/(float)1023;
98      masterduty[enable] = masterintensity[enable]/masterstep[enable];
99
100     void configPWM(float frequency, int duty, int phase, float
        masterfrequency, int masterduty);
101
102 }
```

Listing A.1: Isolation Transformer Code

A.2 Audio Transformer Circuit Code

```
1
2 #include <Arduino.h>
3 #include "stimulation.hpp"
4 #include <driver/ledc.h>
5 #include "config_pins.h"
```

```
#include "global_var.hpp"
#include "Wire.h"

#define STIMULATION_ENABLE_1 32 // Generic GPIO definition
#define STIMULATION_PIN_P_1 33
#define STIMULATION_PIN_N_1 25

void configPWM(float frequency, int duty, int phase, float
    masterfrequency, int masterduty){

        ledc_timer_config_t ledc_timer1 = {   /*Positive and negative
    ulses timer configuration*/
        .speed_mode = (ledc_mode_t) 0,
        {.duty_resolution = LEDC_TIMER_10_BIT},
        .timer_num = (ledc_timer_t) 0,
        .freq_hz = frequency,
        };


        ledc_timer_config_t ledc_timer3 = {   /*Modulator pulse timer
    configuration*/
        .speed_mode = (ledc_mode_t) 0,
        {.duty_resolution = LEDC_TIMER_10_BIT},
        .timer_num = (ledc_timer_t) 1,
        .freq_hz = masterfrequency,
        };


        ledc_channel_config_t ledc_channel1 = {
        .gpio_num       = STIMULATION_PIN_N_1,  /*Negative pulse channel
     configuration*/
        .speed_mode     = (ledc_mode_t) 0,
        .channel        = (ledc_channel_t) 0,
        .intr_type      = (ledc_intr_type_t) LEDC_INTR_DISABLE,
        .timer_sel      = (ledc_timer_t) 0,
```

```
37        .duty           = 0,
38        .hpoint         = 0
39        };
40
41        ledc_channel_config_t ledc_channel2 = { /*Positive pulse channel
     configuration*/
42        .gpio_num       = STIMULATION_PIN_P_1,
43        .speed_mode     = (ledc_mode_t) 0,
44        .channel        = (ledc_channel_t) 1,
45        .intr_type      = (ledc_intr_type_t) LEDC_INTR_DISABLE,
46        .timer_sel      = (ledc_timer_t) 0,
47        .duty           = 0,
48        .hpoint         = 0
49        };
50
51        ledc_channel_config_t ledc_channel5 = { /*Modulator pulse
    channel configuration*/
52        .gpio_num       = STIMULATION_ENABLE_1,
53        .speed_mode     = (ledc_mode_t) 0,
54        .channel        = (ledc_channel_t) 2,
55        .intr_type      = (ledc_intr_type_t) LEDC_INTR_DISABLE,
56        .timer_sel      = (ledc_timer_t) 1,
57        .duty           = 0,
58        .hpoint         = 0
59        };
60
61
62        /*Functions call*/
63
64        ledc_timer_config(&ledc_timer1);
65        ledc_channel_config(&ledc_channel1);
66        ledc_channel_config(&ledc_channel2);
67        ledc_set_duty_with_hpoint((ledc_mode_t)0, (ledc_channel_t)0,
    duty, 0);
```

```
68          ledc_set_duty_with_hpoint((ledc_mode_t)0, (ledc_channel_t)1,
    duty, phase);
69          ledc_update_duty((ledc_mode_t)0, (ledc_channel_t)0);
70          ledc_update_duty((ledc_mode_t)0, (ledc_channel_t)1);
71
72          ledc_timer_config(&ledc_timer3);
73          ledc_channel_config(&ledc_channel5);
74          ledc_set_duty_with_hpoint((ledc_mode_t)0, (ledc_channel_t)2,
    masterduty, 0);
75          ledc_update_duty((ledc_mode_t)0, (ledc_channel_t)2);
76      }
77
78    void stimulation(int I, int P, int F, int enable)
79 {
80
81      period = P;
82      frequency = 1 / (period[enable] / 1000000);
83      step = period/1023; // 10 bits of resolution
84      duty = I;
85      shift = 511; // shift in the half
86
87      masterintensity = period;
88
89      masterfrequency = F;  //1/(masterperiod[enable]/1000000);
90      masterperiod = 1/((float)F/1000000);
91      masterstep = (float)masterperiod / (float)16383;
92      masterduty = masterintensity/masterstep;
93
94      configPWM(frequency, duty, shift, masterfrequency, masterduty);
95 }
```

Listing A.2: Isolation Transformer Code